Published June 21, 2010

JEM

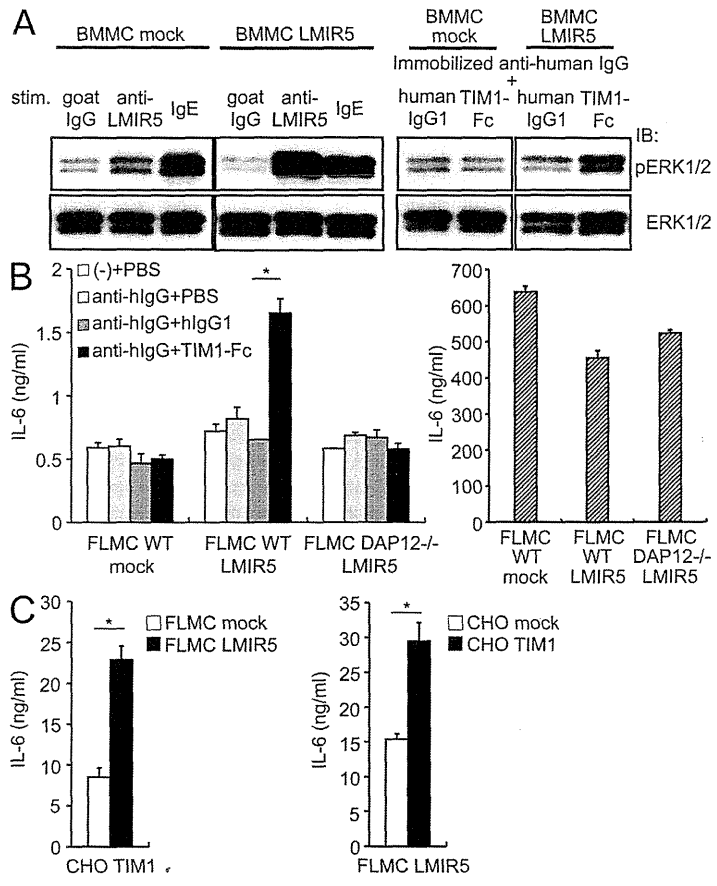

Figure 4. The binding of TIM1 to LMIR5 induced LMIR5-mediated mast cell activation. (A) BMMCs transduced with LMIR5 or mock were stimulated with anti-LMIR5 antibody, goat IgG, or SPE-7 IgE (left), or with TIM1-Fc or human IgG1 (right). Cell lysates were subjected to immunoblotting (IB) with anti-phospho-p44/42 mitogen-activated protein kinase (pERK1/2). One representative out of three independent experiments is shown. (B) Either WT or DAP12-deficient FLMCs transduced with LMIR5 or mock were stimulated with 100 nM PMA (right) or with TIM1-Fc, human IgG1 (hIgG1), or PBS (left). (C) FLMCs transduced with LMIR5 or mock were co-cultured with TIM1-expressing CHO cells (left), or LMIR5-expressing FLMCs were co-cultured with CHO cells transduced with TIM1 or mock for 24 h (right). IL-6 released into the culture supernatants was measured by ELISA. Data are means ± SD of four triplicate samples. One representative out of four independent experiments is shown. Statistically significant differences are shown. *, $P < 0.05$.

compared the IRI kidneys from WT mice with those from LMIR5$^{-/-}$ mice. Flow cytometric analysis delineated that the percentage of neutrophils in IRI kidneys was lower in LMIR5-deficient mice compared with WT mice (Fig. 5 D). On the other hand, in vitro migration assays demonstrated a comparable ability of WT and LMIR5$^{-/-}$ neutrophils to migrate toward chemoattractants such as MIP-2, C5a, KC, and fMLP (Fig. S7 A). To further test if the LMIR5–TIM1 interaction was involved in the neutrophil accumulation in the kidney IRI, we used dorsal air pouch experiments as an in vivo neutrophil recruitment model. Importantly, both TIM1-Fc–induced neutrophil migration and cytokine production in dorsal air pouches were dampened by LMIR5 deficiency, although the response to LPS was comparable between both mice (Fig. 5, E and F). These results suggested that the LMIR5–TIM1 interaction contributed to the accumulation of neutrophils in kidney IRI.

LMIR5 deficiency ameliorates renal tubular damage induced by kidney IRI

Next, we examined if LMIR5 deficiency attenuated the renal damage induced by IRI. As previously reported (Kelly et al., 1996; Wu et al., 2007; Lech et al., 2009), higher amounts of IL-6 and MCP-1 were produced in IRI kidneys compared with contralateral kidneys of WT mice (Fig. 6 A and Fig. S7 B). Notably, LMIR5 deficiency attenuated the increase of cytokine production in IRI kidneys, whereas it did not affect TIM1 expression in IRI kidneys (Fig. 6 A and Fig. S7 B). In WT mice, IL-6 transcripts were equivalently expressed in CD45$^+$ and CD45$^-$ cells of IRI kidneys, whereas MCP-1 transcripts were highly expressed in CD45$^+$ cells (Fig. 6 B). These results indicated a contributory role of CD45$^+$ cells in cytokine/chemokine production of IRI kidneys. Histological analysis of IRI kidneys showed severe tubular damage of WT mice, as indicated by widespread tubular necrosis in the outer medulla and cast formation in the inner medulla at 1 d after IRI (Fig. 6 C). On the other hand, tubular damage was significantly ameliorated by LMIR5 deficiency (Fig. 6 C). Related to this, the number of neutrophils infiltrating the interstitial compartments of IRI kidneys was lower in LMIR5-deficient mice compared with WT mice (Fig. 6, D and E). We found no tubular damage as well as negligible numbers of neutrophils in contralateral kidneys of WT or LMIR5$^{-/-}$ mice (Fig. 6, C and E; and not depicted). Importantly, immunohistological examination displayed the frequent colocalization of LMIR5-expressing neutrophils and TIM1-expressing tubular epithelial cells in IRI kidneys of WT mice (Fig. 6 F). Altogether, LMIR5 deficiency ameliorated ischemia-induced renal tubular damage associated with neutrophil accumulation.

DISCUSSION

Identification of ligands for immune receptors is indispensable for delineation of their biological functions. Recent studies led us to postulate that paired immune receptors have acquired the ability to recognize both endogenous and exogenous ligands (Shiratori et al., 2004; Satoh et al., 2008). The same hypothesis could be applied to LMIR/CD300 family members, but their ligands remained unknown.

Published June 21, 2010

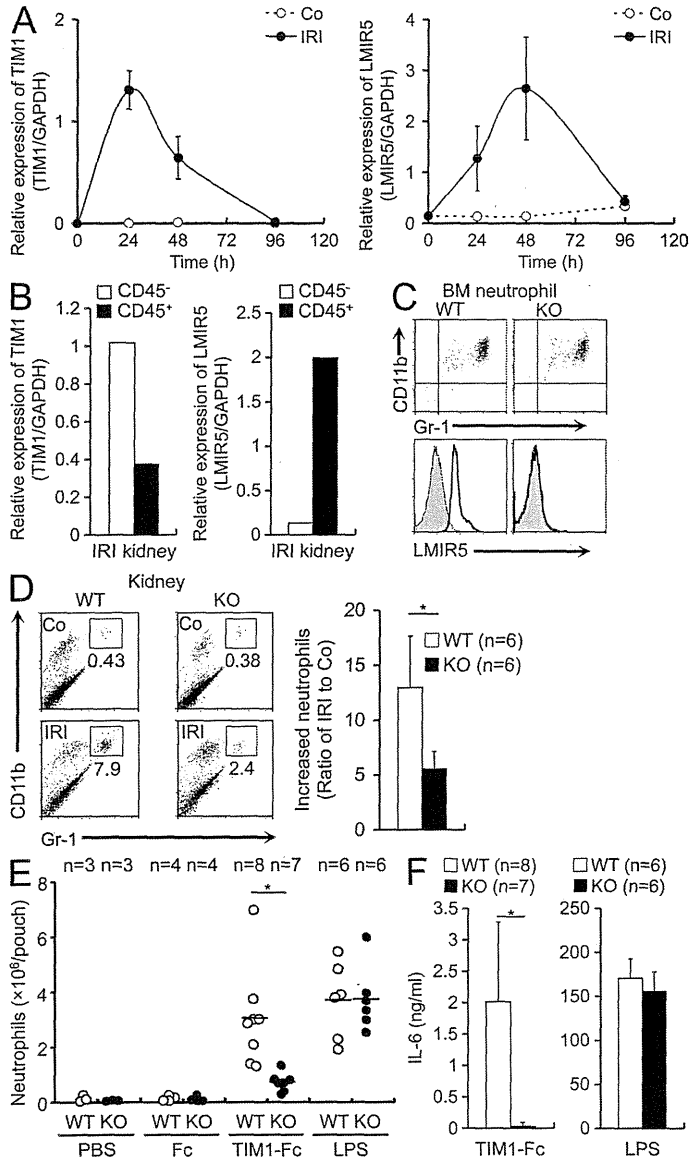

Figure 5. In vivo evidence that the LMIR5–TIM1 interaction induced accumulation of neutrophils. (A and B) Relative gene expression levels of TIM1 (left) or LMIR5 (right) in the IRI or contralateral (Co) kidneys from WT mice at different time intervals after surgery (A) or in the $CD45^-$ or $CD45^+$ cells sorted from the IRI kidneys of WT mice at 24 h after surgery (B). Data are means ± SD ($n = 6$ mice in each group). Data are representative of three independent experiments. (C) Surface expression levels of LMIR5 (bottom, continuous line histograms) as well as CD11b and Gr-1 (top) were examined in BM neutrophils from WT or $LMIR5^{-/-}$ (KO) mice. Control staining with goat IgG is shown (shaded histograms). Data are representative of five independent experiments. (D) Percentages of $CD11b^+Gr\text{-}1^+$ neutrophils in either contralateral or IRI kidney cells from WT or KO mice at 24 h after surgery (left). The ratio of neutrophil counts in IRI kidneys to those in contralateral kidneys was determined. Data are means ± SD ($n = 6$ mice in each group; right). Two independent experiments were performed. (E) Either 100 µg TIM1-Fc or control Fc, or 1 mg LPS was injected into the air pouches of WT or $LMIR5^{-/-}$ mice. At 4 h after injection, neutrophils recruited into the pouches were counted. Each symbol represents an individual mouse. The number of mice in each group is shown. Two independent experiments were performed. (F) IL-6 released into the dorsal air pouches (ELISA). The number of mice in each group is shown. Two independent experiments were performed. Data in D–F are means ± SD. Statistically significant differences are shown. *, $P < 0.05$.

In the present study, we identified TIM1 and TIM4 as endogenous ligands for LMIR5. Because TIM1 and TIM4 play an important role in mediating uptake of apoptotic cells through recognition of PS, we were curious about the specific functions of LMIR5 in a similar context. In fact, the Ig-like domain of LMIR5 bound to TIM1 in the vicinity of the PS-binding site within the Ig-like domain of TIM1 (Fig. 2). However, the LMIR5–TIM1/4 interaction did not hamper the TIM1/4-mediated clearance of apoptotic cells (Fig. 3, C–E). One possible explanation is that TIM1 or TIM4 binds to PS at a higher affinity in comparison to LMIR5. Alternatively, the binding site of TIM1 or TIM4 to LMIR5 might be close, but not identical, to that to PS. In addition, several lines of evidence (Fig. 3, A and B) led us to conclude that LMIR5 is not directly involved in the clearance of apoptotic cells. Because LMIR5 is a DAP12-coupled activating receptor, it is plausible that the LMIR5–TIM1/4 interaction induces activation of LMIR5-expressing mast cells. However, in in vitro experiments, myeloid cells were not activated by the interaction of endogenous LMIR5 and TIM1. As one possible explanation, we assumed that biological events induced by the LMIR5–TIM1 interaction require in vivo environmental factors such as cytokines/chemokines, cell–cell interaction, or cell–extracellular matrix interaction. We also postulated that the biological outcomes induced by the LMIR5–TIM1 interaction might be evident in a pathological situation where soluble TIM1 and/or surface-expressed LMIR5 increase at high levels. To test this, we generated LMIR5-deficient mice and used a mouse model of acute kidney injury, IRI, where TIM1 is up-regulated in the IRI kidney. Intriguingly, LMIR5 deficiency attenuated the acute kidney damage, characterized by tubular necrosis and cast formation. In addition, the recruitment of neutrophils in IRI kidneys, reportedly associated with tissue damage (Kelly et al., 1996; Wu et al., 2007; Bolisetty and Agarwal, 2009; Lech et al., 2009), was suppressed in LMIR5-deficient mice. Notably, IRI induced the marked up-regulation of TIM1 expression in epithelial tubular cells, followed by the recruitment of neutrophils to IRI kidneys. Considering that a large amount of soluble TIM1 is released in the ischemic kidneys, it was possible that LMIR5-expressing myeloid cells interacted with soluble TIM1 or surface TIM1 in

Published June 21, 2010

JEM

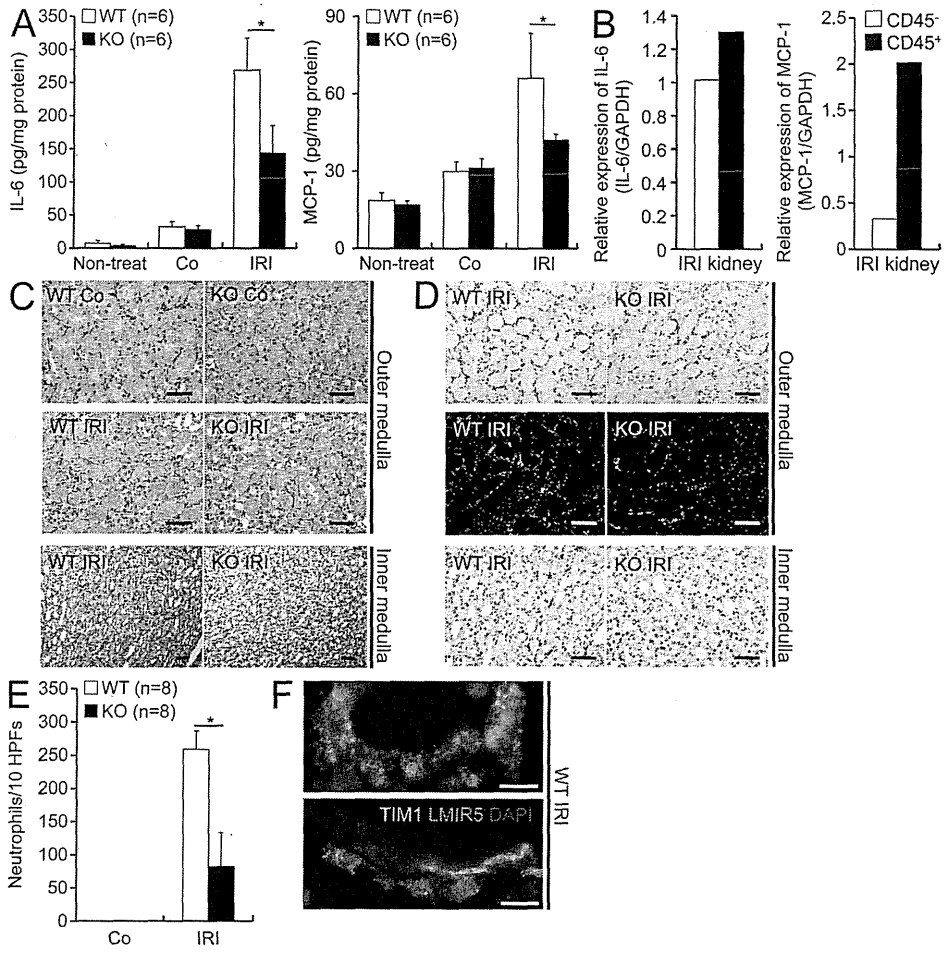

Figure 6. LMIR5$^{-/-}$ mice were protected from renal IRI. (A and B) IL-6 or MCP-1 protein expression (ELISA) in contralateral (Co) or IRI kidneys from WT or LMIR5$^{-/-}$ mice at 24 h after surgery or in nontreated kidneys (A), and relative gene expression levels of IL-6 or MCP-1 (real-time PCR) in CD45$^-$ or CD45$^+$ cells sorted from IRI kidneys at 24 h after surgery (B). Data are means ± SD (n = 6 mice in each group). Statistically significant differences are shown. *, $P < 0.05$. Data are representative of three independent experiments. (C and D) Tubular injury (C) or neutrophil accumulation within the interstitium in IRI kidneys (D) of WT and LMIR5$^{-/-}$ mice at 24 h after surgery. Representative sections of the outer and inner medulla from contralateral or IRI kidneys from WT and LMIR5$^{-/-}$ mice at 24 h after surgery. (C) Hematoxylin and eosin staining. Bars, 100 µm. Three independent experiments were performed. (D) Immunohistochemical identification of neutrophils (brown) in the outer and inner medulla (top and bottom, respectively). Immunohistochemical identification of neutrophils (green) in the outer medulla (middle). The nuclei were counterstained with DAPI (blue). Bars, 100 µm. Three independent experiments were performed. (E) Neutrophil counts of 10 high-power fields (HPFs) from each section from the outer medulla. Data shown are means ± SD (n = 8 mice in each group). Statistically significant differences are shown. *, $P < 0.05$. Three independent experiments were performed. (F) Immunohistochemical identification of LMIR5-expressing neutrophils (red) and TIM1-expressing epithelial cells (green) in the outer medulla of IRI kidneys of WT mice. The nuclei were counterstained with DAPI (blue). Bars, 10 µm. Three independent experiments were performed. ND, not detected.

epithelial cells. In support of this, histological examination displayed the frequent colocalization of LMIR5-expressing neutrophils and TIM1-expressing epithelial cells in IRI kidneys. Taking these observations together, we assume the relevant mechanism to be as follows. First, soluble TIM1 released from or surface TIM1 expressed by renal tubular cells activates LMIR5-expressing myeloid cells, including resident macrophages/monocytes, mast cells, neutrophils, and dendritic cells through the LMIR5–TIM1 interaction. Then, production of cytokines/chemokines and/or soluble TIM1 promotes the neutrophil recruitment, leading to the renal tubular damage. This scenario was supported by the finding that the neutrophil accumulation induced by TIM1-Fc, a mimic form of soluble TIM1, was dampened by LMIR5 deficiency in the dorsal air pouch experiments. Because the migration of BM neutrophils toward chemoattractants was not affected by LMIR5 deficiency in the in vitro assay (Fig. S7 A), we reasoned that the impaired recruitment of neutrophils in LMIR5-deficient mice was presumably caused by the lack of LMIR5–TIM1 interaction, but not to the

Published June 21, 2010

defective migratory function of LMIR5-deficient neutrophils. Of note, neutrophils failed to migrate toward TIM-Fc alone in the in vitro assay (unpublished data), suggesting the requirement of additional signals supplied by the surrounding cells in vivo. We concluded that soluble TIM1 induced the neutrophil accumulation via LMIR5 under in vivo conditions through both direct and indirect mechanisms. However, TIM1-Fc also binds to LMIR5-deficient neutrophils as well as parent Ba/F3 cells (Fig. S1 C and not depicted), suggesting the existence of unidentified ligands for TIM1. Although recent studies implied multiple mechanisms in the pathology of kidney IRI (Kelly et al., 1996; Wu et al., 2007; Bolisetty and Agarwal, 2009; Jang and Rabb, 2009; Lech et al., 2009), the present paper shows that the LMIR5–TIM1 interaction was involved in the tubular damage in the acute phase after IRI.

In conclusion, we provide evidence that TIM1 is a physiological ligand for LMIR5 and that the LMIR5–TIM1 interaction is pivotal in neutrophil accumulation related to tissue damage in kidney IRI. Blocking the LMIR5–TIM1 interaction might be a novel therapeutic strategy for acute renal tubular damage.

MATERIALS AND METHODS

Cells and mice. *DAP12*$^{-/-}$ mice were used as previously described (Kaifu et al., 2003). Animal experiments were conducted in accordance with the guidelines of and with permission provided by the Animal Care and Use Committee of the University of Tokyo (approval no. 20-8). *LMIR5*$^{-/-}$ mice were generated as previously described (Murata et al., 2004). We used *LMIR5*$^{-/-}$ mice that had been backcrossed for at least eight generations with C57BL/6 mice (Charles River).

BM-derived cells, FLMCs, and peritoneal macrophages were generated as previously described (Izawa et al., 2007; Kobayashi et al., 2007; Miyanishi et al., 2007; Yamanishi et al., 2008). Single-cell suspensions of kidney cells were obtained by using Liberase Research Grade Enzyme (Roche).

Antibodies and other reagents. Anti-LMIR5 polyclonal antibody and anti-TIM1 mAb (222414) were obtained from R&D Systems. Biotinylated anti–mouse TIM1 (RMT1-10 or RMT1-4) mAbs were obtained from eBioscience. Anti–mouse TIM1 (RMT1-17), TIM2 (RMT2-14), TIM3 (RMT3-23), and TIM4 (RMT4-54) mAbs have been previously described (Nakayama et al., 2009).

Gene expression analysis. Real-time PCR or RT-PCR was performed using gene-specific primers (Table S1) as previously described (Yamanishi et al., 2008).

Generation of Fc fusion proteins. The cDNA fragments corresponding to the extracellular domains of mouse LMIR1/2/3/4/5, LMIR5 deletion mutants, TIM1, or TIM4 were used. The Fc fusion proteins were purified as previously described (Satoh et al., 2008).

Flow cytometry. In some experiments, cells were stained with 1 μg/ml of Fc fusion proteins or human IgG1 followed by 10 μg/ml of PE-conjugated $F(ab')_2$ donkey anti–human IgG. Flow cytometric analysis was performed with a FACSCalibur (BD) equipped with CellQuest software (BD) and FlowJo software (Tree Star, Inc.), as previously described (Izawa et al., 2007; Yamanishi et al., 2008).

Retrovirus-mediated expression cloning. Expression cloning was performed as previously described (Kitamura et al., 2003). In brief, plasmids (provided by H. Arase, Osaka University, Osaka, Japan) from the cDNA library were transfected into PLAT-E packaging cells (Morita et al., 2000). Infected Ba/F3 cells were stained by LMIR5-Fc. After three rounds of enrichment using a FACSAria (BD), single-cell clones were obtained. The integrated cDNA was recovered by PCR and sequenced.

PIP-strip assay. PIP-strip assay was performed as previously described (Kobayashi et al., 2007). PIP strips were purchased from Echelon Bioscience.

Phagocytosis assay. Phagocytosis assay was performed as previously described (Kobayashi et al., 2007; Miyanishi et al., 2007). CFSE-labeled apoptotic thymocytes were coincubated with peritoneal macrophages in the presence of 10 μg/ml of the Fc fusion proteins indicated in the figures for 30 min. Alternatively, CFSE-labeled live or apoptotic U937 cells were coincubated with NIH3T3 transfectants in the presence of 20 μg/ml of the antibodies or Fc fusion proteins indicated in the figures for 45 min. The percentage of $CSFE^+$ cells was measured by flow cytometric analysis.

Immunoprecipitation and Western blotting. Transfected Ba/F3 cells were incubated with 20 μg/ml LMIR5-Fc, human IgG1, anti-Flag mAb, or mouse IgG1. Cell lysates were immunoprecipitated by using protein A–sepharose. To detect phosphorylation of ERK1/2, transfected BMMCs preincubated with 20 μg/ml TIM1-Fc or human IgG1 for 30 min on ice were stimulated in anti–human IgG antibody–coated plates at 37°C for 7 min, as previously described (Kumagai et al., 2003; Izawa et al., 2007; Yamanishi et al., 2008).

Measurement of cytokines. For co-culture assay, 5×10^4 CHO cells transduced with TIM1 or mock transduced were co-cultured with 2×10^5 FLMCs transduced with LMIR5 or mock transduced for 24 h. Concentrations of IL-6 in the culture supernatants and those of IL-6 and MCP-1 in the renal extract were measured by ELISA, as previously described (Izawa et al., 2007; Wu et al., 2007; Yamanishi et al., 2008). Protein levels of cytokines/chemokines in the renal extract were corrected for the total amounts of protein.

Neutrophil infiltration into mouse dorsal air pouch. Air pouches were formed on the dorsum of mice as previously described (Sin et al., 1986). In brief, 7 ml of sterile air was injected subcutaneously into the back of mice on days 0 and 3. On day 6, 100 μg TIM1-Fc or of control Fc, or 1 mg LPS dissolved in 1 ml of PBS was injected into the air pouches. 4 h after the injection, the air pouches were lavaged. Total cells in the lavage fluid were counted and the percentages of $Gr\text{-}1^+/CD11b^+$ neutrophils were estimated by FACS analysis. IL-6 levels in the lavage fluid were measured by ELISA.

Induction of renal IRI. In brief, the left renal pedicle of male mice was exposed and clamped for 45 min with a microaneurysm clamp via flank incision, as previously described (Lech et al., 2009). Mice were sacrificed at 24, 48, and 96 h after reperfusion. The IRI and contralateral kidneys were collected for histological analysis, flow cytometry analysis, and measurements of cytokines and chemokines.

Histological analysis. Formalin-fixed kidneys were embedded in paraffin and stained with hematoxylin and eosin by standard methods. Neutrophils were detected using rat anti–mouse neutrophil mAb (clone 4/7; AbD Serotec), as previously described (Wu et al., 2007). Neutrophils in the outer medulla were counted in 10 consecutive high-power fields (400×) from each section. Immunofluorescence staining was performed as previously described (Morikawa et al., 2004). In brief, 6-μm-thick frozen sections were stained with primary antibodies: anti-LMIR5 antibody, anti-TIM1 (RMT1-17) mAb, rat anti–mouse neutrophil mAb, and the appropriate secondary antibodies (Jackson ImmunoResearch Laboratories, Inc.). All sections were counterstained with DAPI (Invitrogen).

Statistical analysis. Data are shown as means ± SD. Statistical significance was determined by the Student *t* test, with $P < 0.05$ considered statistically significant.

Published June 21, 2010

JEM

Online supplemental material. Fig. S1 shows that TIM1 was identified as the ligand for LMIR5 by retrovirus-mediated expression cloning. Fig. S2 shows differential blocking effects of anti-TIM1 antibodies on the TIM1–LMIR5 interaction. Fig. S3 shows that TIM4-Fc as well as TIM1-Fc induced LMIR5-mediated activation of mast cells. Fig. S4 shows no detectable expression levels of TIM1 and TIM4 in BMMCs, FLMCs, or neutrophils. Fig. S5 shows gene targeting of *LMIR5*. Fig. S6 shows normal development of myeloid cells and lymphocytes in LMIR5$^{-/-}$ mice. Fig. S7 shows relative gene expression levels of IL-6, MCP-1, TIM1, or LMIR5 in the postischemic kidneys from WT or LMIR5$^{-/-}$ mice. Table S1 shows the gene-specific primers used in this study. Online supplemental material is available at http://www.jem.org/cgi/content/full/jem.20090581/DC1.

We thank Dr. H. Arase for providing plasmids. We also thank Drs. N. Watanabe and Y. Ishi for cell sorting, and K. Kimura for histological analysis. We are grateful to Dr. D. Wylie for her excellent language support.

This study was supported by grants from the Ministry of Education, Culture, Sports, Science, and Technology (MEXT), Japan, and was in part supported by the Global Center of Excellence Program "Center of Education and Research for the Advanced Genome-Based Medicine–for personalized medicine and the control of worldwide infectious diseases," MEXT, Japan. Y. Yamanishi is supported by a postdoctoral fellowship from the Japan Society for the Promotion of Science.

Dr. T. Kitamura serves as a consultant for R&D Systems. The authors declare no further financial conflicts of interest.

Submitted: 13 March 2009
Accepted: 21 May 2010

REFERENCES

Bailly, V., Z. Zhang, W. Meier, R. Cate, M. Sanicola, and J.V. Bonventre. 2002. Shedding of kidney injury molecule-1, a putative adhesion protein involved in renal regeneration. *J. Biol. Chem.* 277:39739–39748. doi:10.1074/jbc.M200562200

Bolisetty, S., and A. Agarwal. 2009. Neutrophils in acute kidney injury: not neutral any more. *Kidney Int.* 75:674–676. doi:10.1038/ki.2008.689

Chung, D.H., M.B. Humphrey, M.C. Nakamura, D.G. Ginzinger, W.E. Seaman, and M.R. Daws. 2003. CMRF-35-like molecule-1, a novel mouse myeloid receptor, can inhibit osteoclast formation. *J. Immunol.* 171:6541–6548.

Ichimura, T., J.V. Bonventre, V. Bailly, H. Wei, C.A. Hession, R.L. Cate, and M. Sanicola. 1998. Kidney injury molecule-1 (KIM-1), a putative epithelial cell adhesion molecule containing a novel immunoglobulin domain, is up-regulated in renal cells after injury. *J. Biol. Chem.* 273:4135–4142. doi:10.1074/jbc.273.7.4135

Ichimura, T., E.J. Asseldonk, B.D. Humphreys, L. Gunaratnam, J.S. Duffield, and J.V. Bonventre. 2008. Kidney injury molecule-1 is a phosphatidylserine receptor that confers a phagocytic phenotype on epithelial cells. *J. Clin. Invest.* 118:1657–1668.

Izawa, K., J. Kitaura, Y. Yamanishi, T. Matsuoka, T. Oki, F. Shibata, H. Kumagai, H. Nakajima, M. Maeda-Yamamoto, J.P. Hauchins, et al. 2007. Functional analysis of activating receptor LMIR4 as a counterpart of inhibitory receptor LMIR3. *J. Biol. Chem.* 282:17997–18008. doi:10.1074/jbc.M701100200

Jang, H.R., and H. Rabb. 2009. The innate immune response in ischemic acute kidney injury. *Clin. Immunol.* 130:41–50. doi:10.1016/j.clim.2008.08.016

Kaifu, T., J. Nakahara, M. Inui, K. Mishima, T. Momiyama, M. Kaji, A. Sugahara, H. Koito, A. Ujike-Asai, A. Nakamura, et al. 2003. Osteopetrosis and thalamic hypomyelinosis with synaptic degeneration in DAP12-deficient mice. *J. Clin. Invest.* 111:323–332.

Kaplan, G., A. Totsuka, P. Thompson, T. Akatsuka, Y. Moritsugu, and S.M. Feinstone. 1996. Identification of a surface glycoprotein on African green monkey kidney cells as a receptor for hepatitis A virus. *EMBO J.* 15:4282–4296.

Kelly, K.J., W.W. Williams Jr., R.B. Colvin, S.M. Meehan, T.A. Springer, J.C. Gutierrez-Ramos, and J.V. Bonventre. 1996. Intercellular adhesion molecule-1-deficient mice are protected against ischemic renal injury. *J. Clin. Invest.* 97:1056–1063. doi:10.1172/JCI118498

Kitamura, T., Y. Koshino, F. Shibata, T. Oki, H. Nakajima, T. Nosaka, and H. Kumagai. 2003. Retrovirus-mediated gene transfer and expression cloning: powerful tools in functional genomics. *Exp. Hematol.* 31:1007–1014.

Kitaura, J., J. Song, M. Tsai, K. Asai, M. Maeda-Yamamoto, A. Mocsai, Y. Kawakami, F.T. Liu, C.A. Lowell, B.G. Barisas, et al. 2003. Evidence that IgE molecules mediate a spectrum of effects on mast cell survival and activation via aggregation of the FcepsilonRI. *Proc. Natl. Acad. Sci. USA.* 100:12911–12916. doi:10.1073/pnas.1735525100

Klesney-Tait, J., I.R. Turnbull, and M. Colonna. 2006. The TREM receptor family and signal integration. *Nat. Immunol.* 7:1266–1273. doi:10.1038/ni1411

Kobayashi, N., P. Karisola, V. Peña-Cruz, D.M. Dorfman, M. Jinushi, S.E. Umetsu, M.J. Butte, H. Nagumo, I. Chernova, B. Zhu, et al. 2007. TIM-1 and TIM-4 glycoproteins bind phosphatidylserine and mediate uptake of apoptotic cells. *Immunity.* 27:927–940. doi:10.1016/j.immuni.2007.11.011

Kuchroo, V.K., D.T. Umetsu, R.H. DeKruyff, and G.J. Freeman. 2003. The TIM gene family: emerging roles in immunity and disease. *Nat. Rev. Immunol.* 3:454–462. doi:10.1038/nri1111

Kuchroo, V.K., V. Dardalhon, S. Xiao, and A.C. Anderson. 2008. New roles for TIM family members in immune regulation. *Nat. Rev. Immunol.* 8:577–580. doi:10.1038/nri2366

Kumagai, H., T. Oki, K. Tamitsu, S.Z. Feng, M. Ono, H. Nakajima, Y.C. Bao, Y. Kawakami, K. Nagayoshi, N.G. Copeland, et al. 2003. Identification and characterization of a new pair of immunoglobulin-like receptors LMIR1 and 2 derived from murine bone marrow-derived mast cells. *Biochem. Biophys. Res. Commun.* 307:719–729. doi:10.1016/S0006-291X(03)01245-2

Lanier, L.L. 2009. DAP10- and DAP12-associated receptors in innate immunity. *Immunol. Rev.* 227:150–160. doi:10.1111/j.1600-065X.2008.00720.x

Lech, M., A. Avila-Ferrufino, R. Allam, S. Segerer, A. Khandoga, F. Krombach, C. Garlanda, A. Mantovani, and H.J. Anders. 2009. Resident dendritic cells prevent postischemic acute renal failure by help of single Ig IL-1 receptor-related protein. *J. Immunol.* 183:4109–4118. doi:10.4049/jimmunol.0900118

Luo, K., W. Zhang, L. Sui, N. Li, M. Zhang, X. Ma, L. Zhang, and X. Cao. 2001. DIgR1, a novel membrane receptor of the immunoglobulin gene superfamily, is preferentially expressed by antigen-presenting cells. *Biochem. Biophys. Res. Commun.* 287:35–41. doi:10.1006/bbrc.2001.5539

McIntire, J.J., S.E. Umetsu, O. Akbari, M. Potter, V.K. Kuchroo, G.S. Barsh, G.J. Freeman, D.T. Umetsu, and R.H. DeKruyff. 2001. Identification of Tapr (an airway hyperreactivity regulatory locus) and the linked Tim gene family. *Nat. Immunol.* 2:1109–1116. doi:10.1038/ni739

Meyers, J.H., S. Chakravarti, D. Schlesinger, Z. Illes, H. Waldner, S.E. Umetsu, J. Kenny, X.X. Zheng, D.T. Umetsu, R.H. DeKruyff, et al. 2005. TIM-4 is the ligand for TIM-1, and the TIM-1–TIM-4 interaction regulates T cell proliferation. *Nat. Immunol.* 6:455–464. doi:10.1038/ni1185

Miyanishi, M., K. Tada, M. Koike, Y. Uchiyama, T. Kitamura, and S. Nagata. 2007. Identification of Tim4 as a phosphatidylserine receptor. *Nature.* 450:435–439. doi:10.1038/nature06307

Morikawa, Y., S. Tamura, K. Minehata, P.J. Donovan, A. Miyajima, and E. Senba. 2004. Essential function of oncostatin m in nociceptive neurons of dorsal root ganglia. *J. Neurosci.* 24:1941–1947. doi:10.1523/JNEUROSCI.4975-03.2004

Morita, S.T.K., T. Kojima, and T. Kitamura. 2000. Plat-E: an efficient and stable system for transient packaging of retroviruses. *Gene Ther.* 7:1063–1066. doi:10.1038/sj.gt.3301206

Murata, T., K. Furushima, M. Hirano, H. Kiyonari, M. Nakamura, Y. Suda, and S. Aizawa. 2004. ang is a novel gene expressed in early neuroectoderm, but its null mutant exhibits no obvious phenotype. *Gene Expr. Patterns.* 5:171–178. doi:10.1016/j.modgep.2004.08.007

Nakae, S., M. Iikura, H. Suto, H. Akiba, D.T. Umetsu, R.H. Dekruyff, H. Saito, and S.J. Galli. 2007. TIM-1 and TIM-3 enhancement of Th2 cytokine production by mast cells. *Blood.* 110:2565–2568. doi:10.1182/blood-2006-11-058800

Nakayama, M., H. Akiba, K. Takeda, Y. Kojima, M. Hashiguchi, M. Azuma, H. Yagita, and K. Okumura. 2009. Tim-3 mediates phagocytosis

of apoptotic cells and cross-presentation. *Blood.* 113:3821–3830. doi:10.1182/blood-2008-10-185884

Ravetch, J.V., and L.L. Lanier. 2000. Immune inhibitory receptors. *Science.* 290:84–89. doi:10.1126/science.290.5489.84

Santiago, C., A. Ballesteros, L. Martínez-Muñoz, M. Mellado, G.G. Kaplan, G.J. Freeman, and J.M. Casasnovas. 2007a. Structures of T cell immunoglobulin mucin protein 4 show a metal-Ion-dependent ligand binding site where phosphatidylserine binds. *Immunity.* 27:941–951. doi:10.1016/j.immuni.2007.11.008

Santiago, C., A. Ballesteros, C. Tami, L. Martínez-Muñoz, G.G. Kaplan, and J.M. Casasnovas. 2007b. Structures of T cell immunoglobulin mucin receptors 1 and 2 reveal mechanisms for regulation of immune responses by the TIM receptor family. *Immunity.* 26:299–310. doi:10.1016/j.immuni.2007.01.014

Satoh, T., J. Arii, T. Suenaga, J. Wang, A. Kogure, J. Uehori, N. Arase, I. Shiratori, S. Tanaka, Y. Kawaguchi, et al. 2008. PILRalpha is a herpes simplex virus-1 entry coreceptor that associates with glycoprotein B. *Cell.* 132:935–944. doi:10.1016/j.cell.2008.01.043

Shiratori, I., K. Ogasawara, T. Saito, L.L. Lanier, and H. Arase. 2004. Activation of natural killer cells and dendritic cells upon recognition of a novel CD99-like ligand by paired immunoglobulin-like type 2 receptor. *J. Exp. Med.* 199:525–533. doi:10.1084/jem.20031885

Sin, Y.M., A.D. Sedgwick, E.P. Chea, and D.A. Willoughby. 1986. Mast cells in newly formed lining tissue during acute inflammation: a six day air pouch model in the mouse. *Ann. Rheum. Dis.* 45:873–877. doi:10.1136/ard.45.10.873

Umetsu, S.E., W.L. Lee, J.J. McIntire, L. Downey, B. Sanjanwala, O. Akbari, G.J. Berry, H. Nagumo, G.J. Freeman, D.T. Umetsu, and R.H. DeKruyff. 2005. TIM-1 induces T cell activation and inhibits the development of peripheral tolerance. *Nat. Immunol.* 6:447–454. doi:10.1038/ni1186

Waanders, F., M.M. van Timmeren, C.A. Stegeman, S.J. Bakker, and H. van Goor. 2010. Kidney injury molecule-1 in renal disease. *J. Pathol.* 220:7–16. doi:10.1002/path.2642

Wu, H., G. Chen, K.R. Wyburn, J. Yin, P. Bertolino, J.M. Eris, S.I. Alexander, A.F. Sharland, and S.J. Chadban. 2007. TLR4 activation mediates kidney ischemia/reperfusion injury. *J. Clin. Invest.* 117:2847–2859. doi:10.1172/JCI31008

Yamanishi, Y., J. Kitaura, K. Izawa, T. Matsuoka, T. Oki, Y. Lu, F. Shibata, S. Yamazaki, H. Kumagai, H. Nakajima, et al. 2008. Analysis of mouse LMIR5/CLM-7 as an activating receptor: differential regulation of LMIR5/CLM-7 in mouse versus human cells. *Blood.* 111:688–698. doi:10.1182/blood-2007-04-085787

Yotsumoto, K., Y. Okoshi, K. Shibuya, S. Yamazaki, S. Tahara-Hanaoka, S. Honda, M. Osawa, A. Kuroiwa, Y. Matsuda, D.G. Tenen, et al. 2003. Paired activating and inhibitory immunoglobulin-like receptors, MAIR-I and MAIR-II, regulate mast cell and macrophage activation. *J. Exp. Med.* 198:223–233. doi:10.1084/jem.20021825

Carcinogenesis vol.31 no.8 pp.1354–1359, 2010
doi:10.1093/carcin/bgq112
Advance Access publication June 4, 2010

Functional screening using a microRNA virus library and microarrays: a new high-throughput assay to identify tumor-suppressive microRNAs

Masashi Izumiya[1,2], Koji Okamoto[3], Naoto Tsuchiya[1] and Hitoshi Nakagama[1,3,*]

[1]Biochemistry Division, National Cancer Center Research Institute, 5-1-1 Tsukiji, Chuo-ku, Tokyo 104-0045, Japan, [2]Department of Gastroenterology, The University of Tokyo Hospital, 7-3-1 Hongo, Bunkyo-ku, Tokyo 113-8655, Japan and [3]Early Oncogenesis Research Project, National Cancer Center Research Institute, 5-1-1 Tsukiji, Chuo-ku, Tokyo 104-0045, Japan

*To whom correspondence should be addressed. Tel: +81 3 3542 2511; Fax: +81 3 3542 2530;
Email: hnakagam@ncc.go.jp

MicroRNA (miRNA) is a class of non-coding RNAs that represses expression of target messenger RNAs posttranscriptionally. A growing body of evidence supports their roles in various normal cellular processes, as well as in pathological conditions, such as cancer. We established a functional screening assay that enables high-throughput identification of miRNAs that have a role in cancer phenotypes of interest, via the combination of pooled lentivirus vectors expressing several hundred miRNA precursors and a custom-made microarray. Self versus self-hybridization analysis using pooled polymerase chain reaction products generated highly linear and reproducible results. To test the feasibility of the assay, we focused on miRNAs that control proliferation of pancreatic cancer cells and successfully identified five miRNAs that negatively control cell proliferation, including miRNA-34a that was previously identified as a representative tumor-suppressive miRNA. The results were further validated using lentivirus vectors expressing each of the five miRNAs or synthetic miRNAs. The function-based nature of the assay enabled identification of miRNAs that were strongly linked to cell proliferation, but the relative ease and flexibility of the assay allow for future studies of cancer stem cells, metastasis and other cancer phenotypes of interest.

Introduction

MicroRNA (miRNA) is a class of evolutionarily conserved non-coding RNAs of ~19 to 22 nucleotides that modulate expression of their target genes posttranscriptionally together with the RNA-induced silencing complex. Since the first identification of *lin*-4 in *Caenorhabditis elegans*, the number of registered miRNAs is expanding and 940 miRNA genes (1100 mature miRNAs) are annotated in humans (miRBase release 15, http://www.mirbase.org/) and more than a thousand miRNA genes are estimated to be located in the human genome (1). Also, contrary to the 'evolutionarily conserved' definition of miRNAs, species-specific miRNAs have been implicated and cloned, suggesting their critical role in the integrity of higher organisms (2). A growing body of evidence suggests that miRNAs have pivotal roles in normal cellular processes (differentiation, proliferation and cell death) and stress response, as well as implicating their involvement in cancer and other pathological conditions (3,4). Indeed, expression profiling studies of miRNA have shown that miRNAs are aberrantly expressed in a variety of cancers (5). Some miRNAs are consistently upregulated or downregulated in cancers, suggesting their possible tumor-promotive or tumor-suppressive features. Moreover, miRNAs were generally downregulated in tumors compared with normal tissues, implicating a multitude of tumor-suppressive miRNAs that have not been fully recognized (5). In light of these facts, the development of functional assays for miRNAs appears to be warranted in order to better elucidate the mechanisms underlying characteristic features of cancer. Here, we have established a high-throughput functional screening assay in which hundreds of miRNAs are characterized after expression of corresponding miRNA precursors via lentivirus vectors. To test the feasibility of the assay, we screened for miRNAs that suppress proliferation of the pancreatic cancer cell line MIA PaCa-2. Five miRNAs were identified, including *microRNA-34a* (*miR-34a*) that was previously reported as one of the p53-responsive miRNAs, with strong tumor-suppressive activity in various cancers (6). Proliferation-suppressive effects of the five miRNAs identified by the new functional screening assay were individually validated by the infection of lentivirus vectors expressing each miRNA precursors. Cooperative data were obtained following transfection of synthetic miRNAs to MIA PaCa-2 cells; flow cytometry revealed that cell cycle arrest was, at least in part, an underlying mechanism for the observed phenotypic effects.

Abbreviations: CDC42, cell division cycle 42 (GTP-binding protein, 25kDa); gDNA, genomic DNA; copGFP, green fluorescent protein (GFP)-like protein from a copepod; miRNA, microRNA; PCR, polymerase chain reaction; PAK1, p21 protein (Cdc42/Rac)-activated kinase 1.

Materials and methods

Cell culture

MIA PaCa-2 cells and 293T cells (ATCC, Manassas, VA) were cultured in Dulbecco's modified Eagle's medium supplemented with 10% fetal bovine serum and 50 U/ml penicillin and 50 μg/ml streptomycin (Invitrogen, Carlsbad, CA). The cells were routinely incubated at 37°C in a humidified atmosphere with 5% CO_2.

Custom-made oligonucleotide microarray

Sequences of miRNA precursors were obtained from Ensembl Genome Browser (Release 55, http://www.ensembl.org) and the UCSC genome browser (hg19, http://genome.ucsc.edu). Oligonucleotide (60mer) probes were designed for 445 miRNA precursors in a Lenti-miR miRNA precursor clone collection (System Biosciences, Mountain View, CA) using eArray software (Agilent Technologies, Santa Clara, CA). All probe sequences were BLAST searched against miRNA precursor sequences using BlastStation2 software (TM Software, Arcadia, CA). The specificity of the probes with the corresponding miRNA precursors was manually checked and probes with poor specificity were replaced with redesigned probes. The custom-made oligonucleotide microarray was designed so that each microarray contains 32 replicates (16 sense and 16 antisense) of specific probes for 445 miRNA precursors on an 8 × 15 k format (Agilent Technologies). Detailed information of the custom-made microarray we designed is available on request.

Infection of lentivirus library into cells and subsequent passages

MIA PaCa-2 cells were seeded at 4×10^5 cells in a six-well dish 1 day prior to viral transduction. A Lenti-miR Virus Library (System Biosciences) and polybrene (hexadimethrine bromide, Sigma–Aldrich, St Louis, MO) at a final concentration of 5 μg/ml were added to the culture medium. Two parallel infections of the Lenti-miR Virus Library (pooled virus library) were performed with a multiplicity of infection of ~3. Cells were incubated at 37°C in a humidified atmosphere for 24 h, after which medium containing the virus library was replaced with Dulbecco's modified Eagle's medium supplemented with 10% fetal bovine serum and antibiotics. Half of the infected cells were transferred to a 10 cm dish and DNA was extracted from the remaining cells (P0). Afterward, cells were cultured in a 10 cm dish and passaged in the proportion of 1:8 when they reached 80–90% confluency. The cells not used for the passage were used for the extraction of DNA. Throughout the screening process, cells were monitored for green fluorescent protein (GFP)-like protein from a copepod (copGFP) by fluorescence microscopy (IX71 Inverted Microscope; Olympus, Tokyo, Japan).

Functional screening assay using the custom-made microarray

Genomic DNA (gDNA) was extracted with a DNeasy Blood and Tissue Kit (Qiagen, Germantown, MD) according to the manufacturer's instructions. miRNA precursors were recovered from gDNA by polymerase chain

reaction (PCR) with specific primers against lentivirus vectors (forward primer: 5′-GCCTGGAGACGCCATCCACGCTG-3′; reverse primer: 5′-GATGTGCGCTCTGCCCACTGAC-3′). The PCR amplicon is a composite of 445 miRNA precursors; each precursor is composed of the stem–loop sequence (defined in the miRBase, ~100 bp) and the flanking genomic regions (~200 bp upstream and downstream) of the miRNA gene, making the total size of the amplicon ~500 to 700 bp (supplementary Figure S1 is available at *Carcinogenesis* Online). Fifty microliter of PCR reaction contained the following final concentrations: 200 ng of gDNA template, 400 μmol/l each of deoxynucleoside triphosphates, 0.3 μM of each PCR primer and 1 U of KOD FX DNA polymerase (Tokyobo, Osaka, Japan). PCR was performed with the following program on a Veriti thermal cycler (Applied Biosystems, Foster City, CA): 94°C for 3 min, 25 cycles of 94°C for 35 s, 65°C for 35 s, 72°C for 1 min and a final step of 72°C for 7 min. Four independent PCR reactions using the same gDNA template were pooled and purified with the Rapid PCR Purification System (Marligen Biosciences, Rockville, MD). Hundred nanogram of purified PCR product were labeled with either Cy3- or Cy5-deoxycytidine triphosphate using a Genomic DNA Enzymatic Labeling Kit (Agilent Technologies) and purified with a Microcon YM-30 Centrifugal Filter Unit (Millipore, Billerica, MA). A pair of Cy3- and Cy5-labeled DNA was combined and hybridized to the custom-made microarray at 65°C and 20 r.p.m. for 24 h in a hybridization oven (Agilent Technologies). Washing of the microarray and data analysis were performed according to the CGH protocol version5.0 (Agilent Technologies). The log ratio of each miRNA precursor was calculated by averaging the log ratio of replicate probes for each miRNA precursor excluding the highest and the lowest values.

Production of pseudovirus particles

Cells (5×10^6 293T) (ATCC) were seeded in a 10 cm dish 1 day prior to transfection and cotransfected with packaging plasmids (pPACKH1-GAG, pPACKH1-REV and pVSV-G) and a vector plasmid containing each miRNA precursor/copGFP (System Biosciences) using Lipofectamine2000 (Invitrogen) according to the manufacturer's instructions. Cells were cultured at 32°C for 48 h in a humidified atmosphere with 5% CO_2, after which culture medium containing pseudovirus particles was collected and stored at −80°C before infection to MIA PaCa-2 cells.

Cell proliferation assay

For the validation using lentivirus vector expressing miRNA precursors, cells were infected with pseudovirus particles using 5 μg/ml of polybrene for 24 h. Cells (0.5×10^4) were subcultured into a 48-well plate after infection, and 3-(4,5-Dimethylthiazol-2-yl)-2,5-diphenyltetrazolium bromide assay was performed using a CellTiter 96 AQueous One Solution Cell Proliferation Assay (Promega, Madison, WI) and a 2030 Arvo *X* 3 multilabel plate reader (PerkinElmer, Waltham, MA) at 3 and 5 days after subculturing. Cells infected with pseudovirus that only express copGFP, but no miRNA precursor (lenti-miR-control), were used as a control of the assay. Expression of miRNA in cells transduced with each miRNA clones was measured by quantitative reverse transcription–polymerase chain reaction prior to 3-(4,5-Dimethylthiazol-2-yl)-2,5-diphenyltetrazolium bromide assay (supplementary method and supplementary Table S2 are available at *Carcinogenesis* Online). For the validation using synthetic mature miRNA, 1×10^4 MIA PaCa-2 cells were subcultured in a 24-well plate and transfected with HiPerfect Transfection Reagent (Qiagen) and 10 nmol/l of Pre-miR miRNA Precursor Molecules (Ambion, Austin, TX). Cells transfected with Pre-miR miRNA Precursor Molecules—Negative Control (Ambion) were used as a control of the assay. Cells were counted every day after transfection up to 5 days using a Countess Automated Cell Counter (Invitrogen) according to the manufacturer's instruction.

Flow cytometric analysis of cell cycle

2×10^5 MIA PaCa-2 cells were plated per 10 cm dish 1 day prior to transfection of synthetic mature miRNAs and incubated at 37°C in a humidified atmosphere with 5% of CO_2 until transfection. Synthetic *miR-29b*, *-34a*, *-222*, *-224*, *-532* and negative control miRNA (Pre-miR, Ambion) were transfected with HiPerfect Transfection Reagent (Qiagen) at a final concentration of 10 nmol/l. Cells were trypsinized and collected at 48 and 72 h after transfection, then fixed with 90% methanol and finally suspended in phosphate-buffered saline(−) with 50 μg/ml of propidium iodide (Sigma–Aldrich), 50 μg/ml of RNase A (Nippon Gene, Tokyo, Japan) and 0.1% fetal bovine serum (Invitrogen). Ten thousand stained cells were analyzed with a FACSCalibur flow cytometer and CellQuest Pro software (BD Biosciences, San Jose, CA) according to the manufacturer's instructions. The proportions of cells in sub-G_1, G_0/G_1, S and G_2/M phase were analyzed with ModFit *LT* software (Verity Software House, Topsham, ME). The averages and standard deviations of cell cycle distributions of MIA PaCa-2 cells transfected with each miRNA were obtained from three biological replicate samples.

Statistical analysis

Pearson product-moment correlation coefficient and standard deviation were calculated using Excel software (Microsoft, Redmond, WA).

Results

Development of a miRNA functional screening assay

To establish a functional screening assay of miRNAs, we employed a pooled lentivirus vector library expressing 445 human miRNA precursors and a custom-made oligonucleotide microarray for the detection of these precursors (Figure 1A). Each lentivirus vector expresses human miRNA precursors together with copGFP, a green fluorescent protein cloned from a copepod, which enables fluorescent microscopic monitoring of cells infected with the vectors (Figure 1B) (7). Although a pooled library is more convenient than individually assessing phenotypic changes of cells infected with each miRNA and is thus suitable for a functional screening assay, it is virtually impossible to screen miRNAs that negatively regulate phenotypes of interest as the number of cells infected with such miRNAs decrease throughout the screening process. We employed a microarray-based approach to the functional screening assay that enables quantification of changes in the copy number of each miRNA precursor to identify miRNAs that negatively as well as positively regulate phenotypes of interest. Briefly, cells infected with a pooled lentivirus vector library undergo phenotypic screening, during which miRNAs that positively or negatively regulate phenotypes of interest are enriched or excluded compared with the original library. miRNAs that generate phenotypes of interest are identified according to the ratio of change in the copy number of each miRNA precursor that is detected by the ratio of differently labeled fluorescent intensity.

In order to assess the linearity of PCR amplification of mixed miRNAs precursors, reproducibility of PCR reactions from two independent experiments was examined (Figure 2A and B). Eight independent PCR amplifications were performed, and two pooled

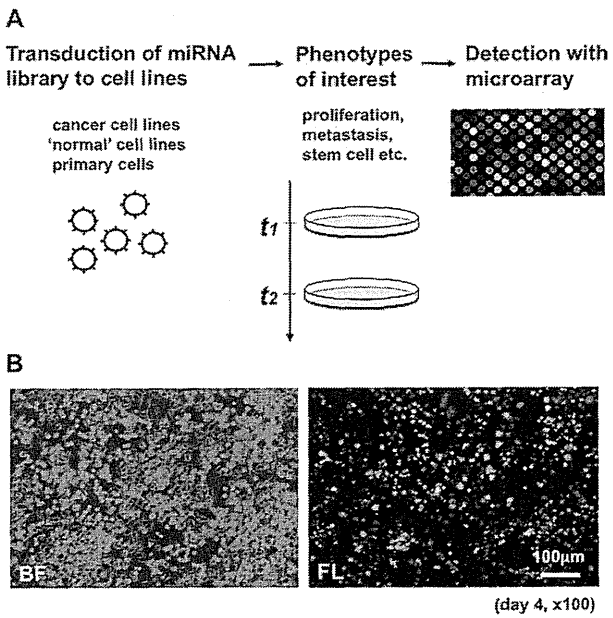

Fig. 1. (**A**) Schematic overview of the functional screening assay of miRNAs. After infection of a pooled lentivirus library (t_1), the phenotypic outcome of each miRNA will be assessed at an appropriate time point (t_2). (**B**) Phase contrast (bright field, BF) and fluorescent (FL) microscopic images of MIA PaCa-2 cells infected with a pooled lentivirus vector library showing copGFP-positive cells.

PCR products, each comprising four PCR reactions (pool I and pool II), were labeled with Cy3- and Cy5-deoxycytidine triphosphate, respectively, and hybridized to the custom-made miRNA oligonucleotide microarray (self versus self-hybridization). We compared the correlation coefficient of pool I and pool II under several PCR conditions, together with the optimized annealing temperature and the number of amplification cycles. A high correlation coefficient for the assay was obtained (R = 0.944, Figure 2B). The correlation coefficient was comparable between PCR products purified by gel electrophoresis or silica membrane (data not shown).

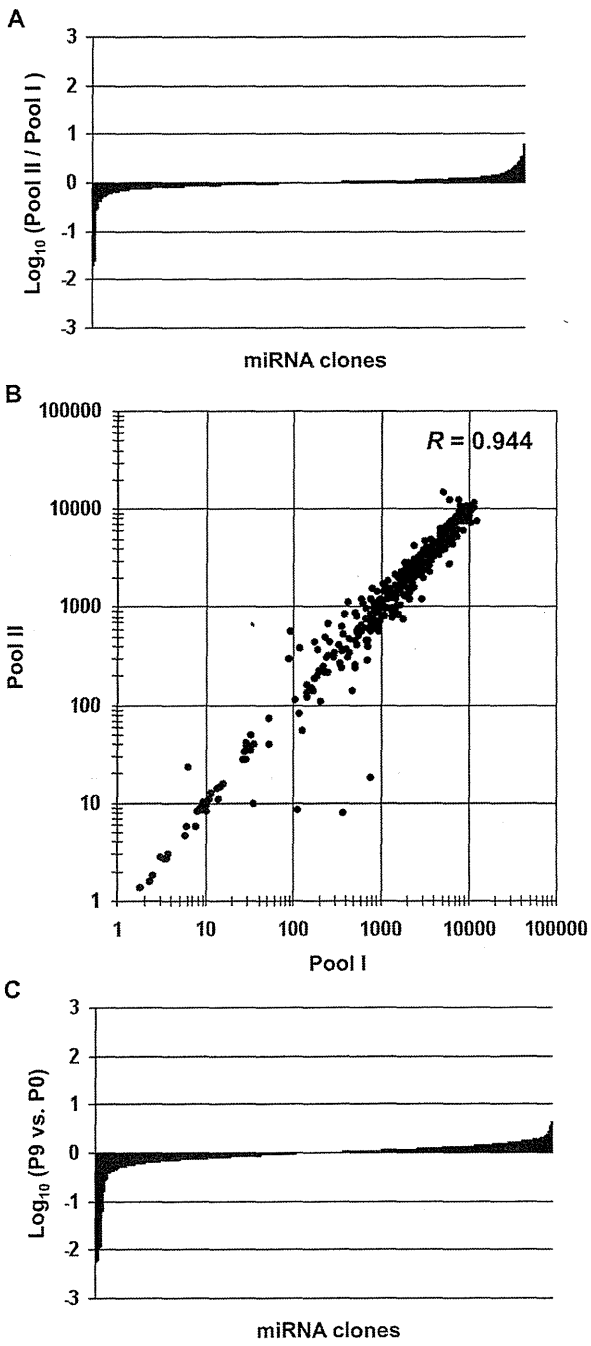

Fig. 2. Distribution of the $\log_{10}$ ratio (**A**) and scatter plot (**B**) of self versus self-microarray hybridization analysis. (**C**) Representative distribution data of the $\log_{10}$ ratio of MIA PaCa-2 cells infected with a pooled lentivirus vector library (P9 versus P0).

Identification of miRNAs that repress proliferation of pancreatic cancer cells

To test the feasibility of the functional screening assay, we focused on the identification of miRNAs that negatively regulate proliferation of human pancreatic cancer cells. MIA PaCa-2 cells were infected with a pooled lentivirus library of miRNA-expressing vectors and passaged several times, during which the expression of miRNA precursors in a majority of cells was confirmed via microscopic inspection of the expression of copGFP (Figure 1B). gDNA was extracted from cells not used for the passage and integrated miRNA precursors were amplified by PCR. Subsequently, amplified miRNA precursors were labeled with Cy3- or Cy5-deoxycytidine triphosphate and hybridized to custom-made microarrays. Any change in the relative proportion of cells expressing each miRNA precursor were measured by comparing labeled miRNAs from cells passaged nine times (P9) and cells immediately after infection (P0) (Figure 2C; supplementary Table S1 is available at *Carcinogenesis* Online). We focused on five miRNAs, namely *miR-29b*, *-34a*, *-222*, *-224* and *-532*, which consistently showed a remarkably low log ratio in two independent screening assays (Table I) and individually validated the proliferation-suppressive phenotypes either using lentivirus vector expressing miRNA precursors, which are components of the pooled virus library used in the functional screening or synthetic mature miRNAs. MIA PaCa-2 cells infected with lentivirus vectors expressing each positive miRNA significantly suppressed cell proliferations (Figure 3A). Moreover, transfection of synthetic *miR-29b*, *-34a*, *-222*, *-224* and *-532* also suppressed proliferation of MIA PaCa-2 cells in comparison with cells transfected with negative control miRNAs. (Figure 3B and C). The fold changes in the expression of the five proliferation-suppressive miRNAs showed variations according to the endogenous expression level of these miRNAs and the titers of the lentivirus vectors transduced (supplementary Table S2 is available at *Carcinogenesis* Online).

Induction of cell cycle arrest after transfection of proliferation-suppressive miRNAs

To gain further insight into the proliferation-suppressive effects of these five miRNAs, flow cytometric analysis was performed using MIA PaCa-2 cells 48 and 72 h after transfection with synthetic miRNAs (Figure 4; supplementary Figure S2 is available at *Carcinogenesis* Online). MIA PaCa-2 cells transfected with *miR-34a*, *-224* and *-532* showed an increased proportion of G_0/G_1 phase in comparison with cells transfected with negative control miRNA, whereas the proportion of G_2/M phase was increased in cells transfected with *miR-222*. No prominent change in cell cycle was observed in MIA PaCa-2 cells transfected with *miR-29b*. A marked increase in the proportion of the sub-G_1 fraction was not observed in MIA PaCa-2 cells transfected with any of the five proliferation-suppressive miRNAs.

Table I. Top five ranked miRNAs that suppress proliferation of MIA PaCa-2 cells

miRNA clones	Mean $\log_{10}$ ratio of two independent screenings (P9 versus P0)
miR-532	−1.668
miR-224	−1.639
miR-29b	−1.211
miR-34a	−1.153
miR-222	−0.970

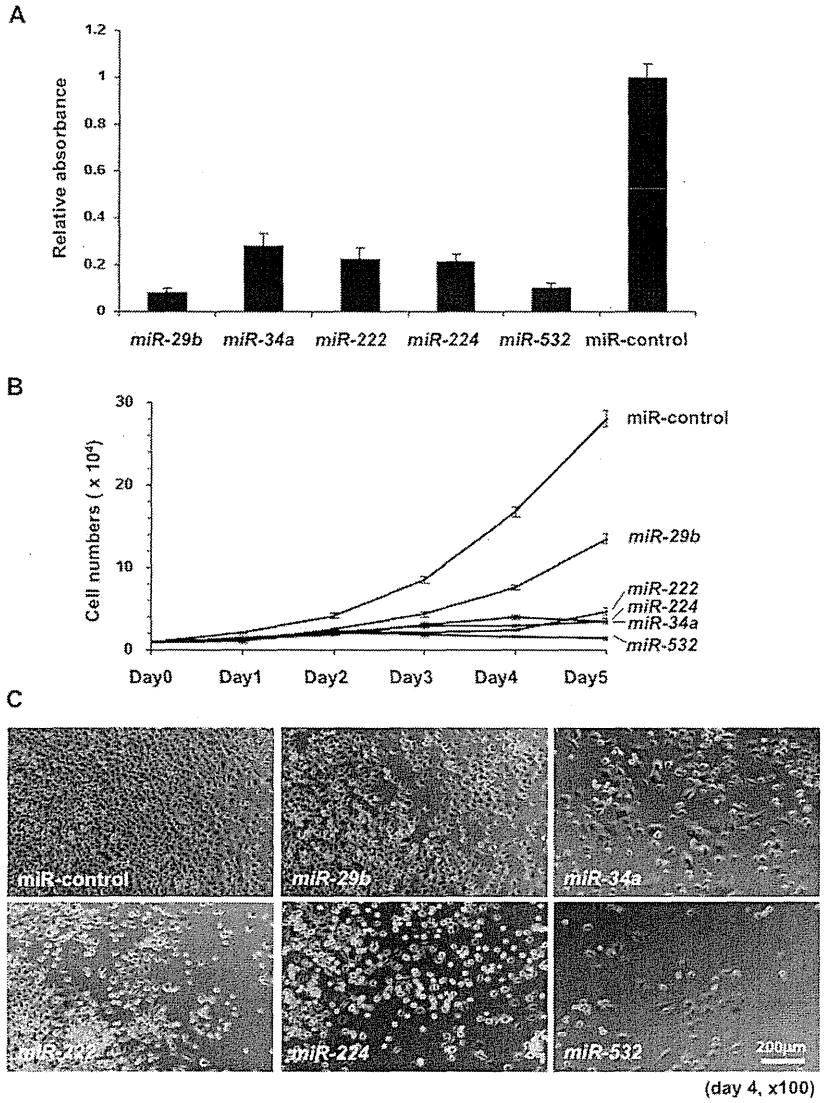

Fig. 3. Cell proliferation assays of MIA PaCa-2 cells. (**A**) 3-(4,5-Dimethylthiazol-2-yl)-2,5-diphenyltetrazolium bromide assay of MIA PaCa-2 cells 5 days after infection with lentivirus vectors expressing miRNA, (**B**) Cell proliferation curve and (**C**) Phase contrast micrographs 4 days after transfection with synthetic miRNAs.

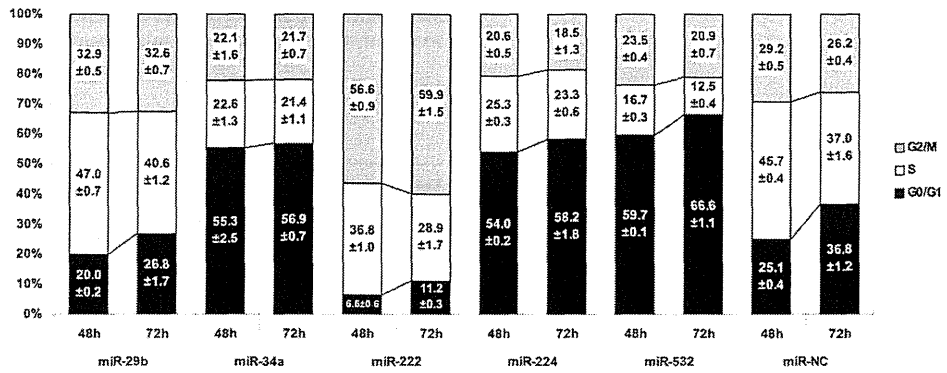

Fig. 4. Distribution of cell cycle phases of MIA PaCa-2 cells 48 and 72 h after transfection with synthetic *miR-29b*, *-34a*, *-222*, *-224*, *-532* and miR-negative control (miR-NC). The average ± standard deviations of three biological replicate samples are shown.

Discussion

A growing body of evidence supports the critical roles of miRNAs in a variety of normal cellular processes, including cell proliferation, cell death and development (3,4). Comprehensive profiling studies have revealed aberrant expression of miRNAs in various pathological conditions, suggesting that miRNAs have a role in the pathogenesis of some diseases, such as cancer. There is increasing interest in miRNA as therapeutic targets, as well as in the application of miRNA as therapeutic agents (5,8). The identification of *miR-34a*, which is transactivated by p53 and represses cell proliferation both *in vitro* and *in vivo*, prompted us to develop an assay to systematically screen for miRNAs that are directly linked to phenotypes characteristic of cancer cells (6). We combined lentivirus vectors expressing miRNA precursors and a custom-made microarray, which we used to monitor the number of lentiviral integrations based on specific sequences within the Lenti-miR virus library.

The usefulness and advantages of such a functional screening approach has recently been shown using a retrovirus vector library expressing short hairpin RNA for several thousand genes, although these short hairpin RNAs are only targeted to knockdown protein-coding genes (9–11). Voorhoeve *et al.* (12) have also constructed a genetic screening assay of miRNAs using a retrovirus vector library (miR-Lib) expressing miRNA minigenes and a barcode microarray (miR-Array). These phenotype-based approaches enabled identification of essential genes critical in cell proliferation that do not necessarily have mutated sequences or aberrant copy numbers and that do not exhibit significantly altered gene expression. Together with the aforementioned assays, the functional screening assay presented here would be a powerful complementary tool for the elucidation and identification of genes critical in establishing the phenotypic characteristics of cancers. By employing lentivirus vectors, we can perform the functional screening assay using non-dividing cells, including stem cells and neural cells, thus broadening the potential application of the assay.

The feasibility of our assay was shown by the successful identification of miRNAs that suppress proliferation of MIA PaCa-2 pancreatic cancer cell lines. We individually validated the proliferation-suppressive effect of the miRNAs that showed significant reduction in their copy numbers in our functional screening assays by transfection of synthetic miRNAs or transduction using lentivirus vectors (Figure 3). Although the fold changes in the expression of these miRNAs in comparison with the endogenous counterpart showed variations, the proliferation-suppressive effect of these miRNAs was at least evident under our experimental conditions (supplementary Table S2 is available at *Carcinogenesis* Online). Interestingly, *miR-34a*, a representative tumor-suppressive miRNA, was identified in the functional screening assay. *miR-34a* is located on chromosome 1p36, which is frequently lost in a variety of cancers (13–17). p53 is one of the factors transactivating *miR-34a*, and it also upregulates p53, suggesting a positive feedback loop formed by p53 and *miR-34a* (18,19). When introduced to cells, *miR-34a* strongly repressed proliferation of colon cancer cell lines HCT116 and RKO, and the cells underwent apoptosis or a premature-senescence phenotype depending on the experimental conditions (18,20–23). Topical application of *miR-34a* also inhibited growth of HCT116 cell lines transplanted to nude mice, implicating *miR-34a* as a potential novel therapeutic agent (18). The precise role of *miR-34a* in pancreatic cancers is still unclear, though its expression is downregulated in most pancreatic cancer cell lines (24). The present functional assay supports a tumor-suppressive role for *miR-34a* in pancreatic cancers, warranting further *in vivo* validation studies of this miRNA using mouse models of pancreatic cancers.

Besides *miR-34a*, we identified four candidate tumor-suppressive miRNAs in pancreatic cancers, namely *miR-29b*, *-222*, *-224* and *-532*. Although a detailed function analysis of these miRNAs is beyond the scope of this study, flow cytometric analysis revealed changes in the distribution of cell cycle phases of MIA PaCa-2 cells transfected with *miR-222*, *-224* and *-532*. Thus, cell cycle arrest is, at least in part, an underlying mechanism of the proliferation-suppressive effect of these miRNAs. Among the predicted targets of these miRNAs are cell division cycle 42 (GTP-binding protein, 25kDa) (CDC42) (*miR-224* and *-532*) and p21 protein (Cdc42/Rac)-activated kinase 1 (PAK1) (*miR-222*) (25–28). CDC42 is a small-guanosine triphosphatase of the Rho-subfamily that contributes to G_1–S phase progression through p70 S6 kinase-mediated induction of cyclin E expression, suggesting the possible role of *miR-224* and *-532* in G_1 arrest through translational suppression of CDC42 (29,30). PAK1 is a serine/threonine p21-actived kinase and is the downstream effector of CDC42 and Rho (31). Knockdown of PAK1 in gastric cancer cells exhibited an increased proportion of cells in G_2/M phase, indicating the possible role of *miR-222* in G_2 arrest through translational suppression of PAK1 (32). Whereas cell cycle arrest was evident in MIA PaCa-2 cells transfected with *miR-222*, *-224* and *-532*, *miR-29b* apparently suppresses cell proliferation through other mechanisms. Park *et al.* (33) reported that *miR-29b* upregulates p53 levels through suppression of p85α and CDC42. Although *TP53* is mutated in MIA PaCa-2 cells (R248W), the combination of suppression of p85α and CDC42 may synergistically confer a proliferation-suppressive phenotype independent of p53.

In conclusion, we have developed a functional screening assay of miRNAs by the combination of a pooled lentivirus library expressing miRNA precursors and a custom-made microarray. The feasibility of the assay was shown by the successful identification of miRNAs that suppress proliferation of MIA PaCa-2 pancreatic cancer cells. Flow cytometric analysis revealed that cell cycle arrest was, at least in part, the underlying mechanism of proliferation-suppressive effects of *miR-34a*, *-222*, *-224* and *-532*. The flexible nature of the assay should facilitate its use in the identification of miRNAs that are involved in a wide array of cancer phenotypes, including cancer stem cells or metastasis.

Supplementary material

Supplementary Tables S1 and S2 and Figures S1 and S2 can be found at http://carcin.oxfordjournals.org/

Funding

Grant-in-Aid for Young Scientists from the Ministry of Education, Culture, Sports, Science, and Technology of Japan (21790694) to MI; Grant-in-Aid for Cancer Research for the Third-Term Comprehensive 10-Year Strategy for Cancer Control from the Ministry of Health, Labour and Welfare of Japan (22090101) to HN; the Program for Promotion of Fundamental Studies in Health Sciences of the National Institute of Biomedical Innovation (08-2) to HN.

Acknowledgements

The authors are grateful to Dr Roderick Dashwood, the Linus Pauling Institute at Oregon State University, for critical reading of the manuscript.

Conflict of Interest Statement: None declared.

References

1. Takada,S. *et al.* (2007) Profiling of microRNA expression by mRAP. *Nat. Protoc.*, **2**, 3136–3145.
2. Berezikov,E. *et al.* (2006) Diversity of microRNAs in human and chimpanzee brain. *Nat. Genet.*, **38**, 1375–1377.
3. Ambros,V. (2004) The functions of animal microRNAs. *Nature*, **431**, 350–355.
4. Kloosterman,W.P. *et al.* (2006) The diverse functions of microRNAs in animal development and disease. *Dev. Cell*, **11**, 441–450.
5. Lu,J. *et al.* (2005) MicroRNA expression profiles classify human cancers. *Nature*, **435**, 834–838.
6. He,L. *et al.* (2007) microRNAs join the p53 network—another piece in the tumour-suppression puzzle. *Nat. Rev. Cancer*, **7**, 819–822.
7. Shagin,D.A. *et al.* (2004) GFP-like proteins as ubiquitous metazoan superfamily: evolution of functional features and structural complexity. *Mol. Biol. Evol.*, **21**, 841–850.

8. Waldman,S.A. *et al.* (2009) A study of microRNAs in silico and *in vivo*: diagnostic and therapeutic applications in cancer. *FEBS J.*, **276**, 2157–2164.
9. Luo,B. *et al.* (2008) Highly parallel identification of essential genes in cancer cells. *Proc. Natl Acad. Sci. USA*, **105**, 20380–20385.
10. Schlabach,M.R. *et al.* (2008) Cancer proliferation gene discovery through functional genomics. *Science*, **319**, 620–624.
11. Silva,J.M. *et al.* (2008) Profiling essential genes in human mammary cells by multiplex RNAi screening. *Science*, **319**, 617–620.
12. Voorhoeve,P.M. *et al.* (2006) A genetic screen implicates miRNA-372 and miRNA-373 as oncogenes in testicular germ cell tumors. *Cell*, **124**, 1169–1181.
13. Praml,C. *et al.* (1995) Deletion mapping defines different regions in 1p34.2-pter that may harbor genetic information related to human colorectal cancer. *Oncogene*, **11**, 1357–1362.
14. White,P.S. *et al.* (1995) A region of consistent deletion in neuroblastoma maps within human chromosome 1p36.2-36.3. *Proc. Natl Acad. Sci. USA*, **92**, 5520–5524.
15. Yeh,S.H. *et al.* (1994) Frequent genetic alterations at the distal region of chromosome 1p in human hepatocellular carcinomas. *Cancer Res.*, **54**, 4188–4192.
16. Nomoto,S. *et al.* (2000) Frequent allelic imbalance suggests involvement of a tumor suppressor gene at 1p36 in the pathogenesis of human lung cancers. *Genes Chromosomes Cancer*, **28**, 342–346.
17. Bieche,I. *et al.* (1999) Deletion mapping of chromosomal region 1p32-pter in primary breast cancer. *Genes Chromosomes Cancer*, **24**, 255–263.
18. Tazawa,H. *et al.* (2007) Tumor-suppressive miR-34a induces senescence-like growth arrest through modulation of the E2F pathway in human colon cancer cells. *Proc. Natl Acad. Sci. USA*, **104**, 15472–15477.
19. Yamakuchi,M. *et al.* (2008) miR-34a repression of SIRT1 regulates apoptosis. *Proc. Natl Acad. Sci. USA*, **105**, 13421–13426.
20. He,L. *et al.* (2007) A microRNA component of the p53 tumour suppressor network. *Nature*, **447**, 1130–1134.
21. Raver-Shapira,N. *et al.* (2007) Transcriptional activation of miR-34a contributes to p53-mediated apoptosis. *Mol. Cell*, **26**, 731–743.
22. Chang,T.C. *et al.* (2007) Transactivation of miR-34a by p53 broadly influences gene expression and promotes apoptosis. *Mol. Cell*, **26**, 745–752.
23. Tarasov,V. *et al.* (2007) Differential regulation of microRNAs by p53 revealed by massively parallel sequencing: miR-34a is a p53 target that induces apoptosis and G1-arrest. *Cell Cycle*, **6**, 1586–1593.
24. Ji,Q. *et al.* (2009) MicroRNA miR-34 inhibits human pancreatic cancer tumor-initiating cells. *PLoS One*, **4**, e6816.
25. Grimson,A. *et al.* (2007) MicroRNA targeting specificity in mammals: determinants beyond seed pairing. *Mol. Cell*, **27**, 91–105.
26. John,B. *et al.* (2004) Human microRNA targets. *PLoS Biol.*, **2**, e363.
27. Krek,A. *et al.* (2005) Combinatorial microRNA target predictions. *Nat. Genet.*, **37**, 495–500.
28. Lewis,B.P. *et al.* (2005) Conserved seed pairing, often flanked by adenosines, indicates that thousands of human genes are microRNA targets. *Cell*, **120**, 15–20.
29. Chou,M.M. *et al.* (2003) Cdc42 promotes G1 progression through p70 S6 kinase-mediated induction of cyclin E expression. *J. Biol. Chem.*, **278**, 35241–35247.
30. Sinha,S. *et al.* (2008) Cellular signaling for activation of Rho GTPase Cdc42. *Cell. Signal.*, **20**, 1927–1934.
31. Dummler,B. *et al.* (2009) Pak protein kinases and their role in cancer. *Cancer Metastasis Rev.*, **28**, 51–63.
32. Liu,F. *et al.* (2009) Downregulation of p21-activated kinase-1 inhibits the growth of gastric cancer cells involving cyclin B1. *Int. J. Cancer*, **125**, 2511–2519.
33. Park,S.Y. *et al.* (2009) miR-29 miRNAs activate p53 by targeting p85 alpha and CDC42. *Nat. Struct. Mol. Biol.*, **16**, 23–29.

Received November 9, 2009; revised May 27, 2010; accepted May 29, 2010

Cancer Cell

A Higher-Order Complex Containing AF4 and ENL Family Proteins with P-TEFb Facilitates Oncogenic and Physiologic MLL-Dependent Transcription

Akihiko Yokoyama,[1,*] Min Lin,[2] Alpana Naresh,[2] Issay Kitabayashi,[1] and Michael L. Cleary[2,*]
[1]Molecular Oncology Division, National Cancer Center Research Institute, Tokyo 104-0045, Japan
[2]Department of Pathology, Stanford University School of Medicine, Stanford, CA 94305, USA
*Correspondence: ayokoyam@ncc.go.jp (A.Y.), mcleary@stanford.edu (M.L.C.)
DOI 10.1016/j.ccr.2009.12.040

SUMMARY

AF4 and ENL family proteins are frequently fused with MLL, and they comprise a higher order complex (designated AEP) containing the P-TEFb transcription elongation factor. Here, we show that AEP is normally recruited to MLL-target chromatin to facilitate transcription. In contrast, MLL oncoproteins fused with AEP components constitutively form MLL/AEP hybrid complexes to cause sustained target gene expression, which leads to transformation of hematopoietic progenitors. Furthermore, MLL-AF6, an MLL fusion with a cytoplasmic protein, does not form such hybrid complexes, but nevertheless constitutively recruits AEP to target chromatin via unknown alternative mechanisms. Thus, AEP recruitment is an integral part of both physiological and pathological MLL-dependent transcriptional pathways. Bypass of its normal recruitment mechanisms is the strategy most frequently used by MLL oncoproteins.

INTRODUCTION

Leukemia is a heterogeneous disease with distinctive biological and clinical properties that are conferred by a variety of acquired genetic mutations (Gilliland, 2002). Chromosomal translocations of the *MLL* gene account for 5%–10% of acute leukemias and are generally associated with poor prognosis (Daser and Rabbitts, 2004; Krivtsov and Armstrong, 2007; Pui et al., 2004). *MLL* gene rearrangements create fusion genes that contain the 5′ portion of *MLL* and the 3′ portion of its fusion partner, whose products cause sustained expression of MLL target genes and consequent enhanced proliferation of hematopoietic progenitors (Ayton and Cleary, 2003; Lavau et al., 1997; Cozzio et al., 2003). The amino-terminal portion of MLL serves as a targeting unit to direct MLL oncoprotein complexes to their target loci through DNA binding (Ayton et al., 2004; Slany et al., 1998) and association with menin and LEDGF (Yokoyama et al., 2005; Yokoyama and Cleary, 2008), whereas the fusion partner portion serves as an effecter unit that causes sustained transactivation (Cheung et al., 2007; Lavau et al., 2000; DiMartino et al., 2000; 2002; Slany et al., 1998; So and Cleary, 2002; 2003). To date, approximately 50 different fusion partners have been reported to form chimeric MLL oncoproteins (Huret et al., 2001). However, the mechanisms underlying this molecular diversity have not been revealed.

The AF4 and ENL protein families are the most frequent MLL fusion partners, accounting for two-thirds of *MLL*-associated leukemia incidence (Huret et al., 2001). The AF4 family comprises four paralogous proteins, including AF4, AF5q31, LAF4, and FMR2. The ENL family includes ENL and AF9 and has structural homology to the yeast Anc1 protein. The members of both protein families possess transactivation domains and therefore are thought to be involved in transcriptional regulation (Prasad et al., 1995; Ma and Staudt, 1996; Morrissey et al., 1997; Slany et al., 1998). All but *FMR2* have been reported to form fusion genes with *MLL* in leukemia (Domer et al., 1993; Taki

Significance

MLL is fused by chromosomal translocations in 5%–10% of acute leukemias to a variety of partner proteins (>50) of diverse molecular composition and function. Recent studies show that several of the more common MLL fusion partners (e.g., AF4, ENL, and AF9) associate in a higher-order complex containing transcription elongation factors. Here we show that this complex is biochemically distinct from the MLL histone methyltransferase complex, but nevertheless normally present at MLL target genes during physiologic gene expression. In acute leukemias, the complex is constitutively recruited to target chromatin by covalent fusion of MLL with one of several complex components or noncovalent mechanisms used by other MLL fusion proteins, thereby representing a unifying mechanism for MLL-mediated leukemogenesis that can be targeted by molecular therapy.

et al., 1999; von Bergh et al., 2002; Iida et al., 1993; Nakamura et al., 1993; Tkachuk et al., 1992). AF4 family proteins associate with ENL family proteins and P-TEFb (Positive Transcription Elongation Factor b) (Erfurth et al., 2004; Zeisig et al., 2005; Bitoun et al., 2007; Mueller et al., 2007). P-TEFb is composed of CDK9 and cyclin T1 (or cyclin T2) and is capable of phosphorylating the carboxy-terminal domain (CTD) of RNA polymerase II (RNAPII) and DSIF to facilitate transcriptional elongation (Saunders et al., 2006; Peterlin and Price, 2006). AF4 functions as a positive regulator of P-TEFb kinase (Bitoun et al., 2007), which, in turn, controls the transactivation activity or stability of AF4 and ENL family proteins. ENL family proteins also associate with DOT1L (Bitoun et al., 2007; Mueller et al., 2007; Zhang et al., 2006), the major histone methyltransferase responsible for the H3K79 methylation mark (Jones et al., 2008), which is predominantly associated with actively transcribed genes (Steger et al., 2008). It has been reported that DOT1L also associates with MLL-AF10 and plays a critical role in its oncogenic transformation (Okada et al., 2005). However, the molecular roles of these components in MLL-dependent leukemogenesis have not been clearly defined.

In this study, we investigated the contributions of a higher order complex containing AF4 and ENL family proteins with P-TEFb in physiologic and pathologic MLL-dependent transcription.

RESULTS

AF4 Forms a Higher Order Complex with AF5q31, ENL, and P-TEFb in Hematopoietic Cells

To identify AF4-associated proteins in vivo, we biochemically purified AF4 complexes from K562 cells using column chromatography followed by immuno-affinity purification with a highly specific anti-AF4 monoclonal antibody (Figure 1A). Mass spectrometry identified AF5q31, ENL, CDK9, and cyclin T1 in the purified materials (Figure 1B). Reciprocal immunoprecipitation (IP) further confirmed that all five proteins compose an endogenous bona fide complex (Figure 1C) consistent with previous observations (Erfurth et al., 2004, Zeisig et al., 2005; Bitoun et al., 2007; Mueller et al., 2007). In gel filtration analysis, the AF4 complex components codistributed in fractions that eluted at an average mass of ~0.8 MDa (Figure 1D). A similar complex was obtained using a monoclonal antibody specific for AF5q31 in the immunoaffinity step (see Figure S1A available with this article online). However, neither purification process yielded other proteins previously reported to interact with ENL (e.g., DOT1L and AF10) (Zeisig et al., 2005; Bitoun et al., 2007; Mueller et al., 2007). These data demonstrate that AF4, AF5q31, and ENL associate in an endogenous higher-order complex (hereafter referred to as "AEP" for the AF4 family/ENL family/P-TEFb complex) containing P-TEFb in hematopoietic lineage cells.

Leukemogenic Fusion Proteins Inappropriately Tether AEP Components with MLL

Co-IP analyses were performed to determine whether MLL chimeric oncoproteins participate in higher-order associations that recapitulate the composition of AEP. Reciprocal IP using human leukemia cell lines that express MLL-ENL, MLL-AF4, or MLL-AF5q31 showed that the respective fusion proteins form similar AEP-like complexes (Figure 1E and Figure S1B). Conversely, MLL-AF6, an MLL fusion with a cytoplasmic protein that was not copurified with AF4 or AF5q31, did not coprecipitate any of the AEP components in ML-2 cells (Figure 1E). Similarly, wild-type (WT) MLL did not pull down AEP components in K562 cells while coprecipitating menin, a component of the MLL complex (Yokoyama et al., 2004) (Figure 1C). Therefore, the MLL and AEP complexes are separate biochemical entities that are inappropriately tethered to form MLL/AEP hybrid complexes by a subset of covalent fusions of MLL in human leukemia cells.

MLL-ENL and MLL-AF4 Consistently Recruit AEP Components to MLL Target Genes

Genomic localizations of MLL chimeric proteins and AEP components were analyzed by chromatin immunoprecipitation (ChIP) in human leukemia cell lines. Histone marks indicative of open chromatin states (tri-methyl H3K4 and acetyl H3K9) (Li et al., 2007) were associated with transcriptionally active loci, whereas histone marks indicative of closed chromatin (di-methyl H3K9 and high levels of histone H3) were associated with transcriptionally inactive loci (Figures 2A–2C), verifying the integrity of ChIP assays. In HB1119 cells, MLL-ENL specifically colocalized with AF4 and AF5q31 at promoter-adjacent regions of the *HOXA9* and *MEIS1* genes, which are known to serve critical roles in MLL-associated leukemogenesis (Ayton and Cleary, 2003; Nakamura et al., 1996; Wong et al., 2007), whereas the presence of AEP at non-MLL target loci such as *β-ACTIN* and *GAPDH* was minimal or negligible (Figure 2B and Figure S2A). Similarly, ChIP analysis showed that AF5q31 and ENL colocalized with endogenous MLL-AF4 on the *HOXA9* and *MEIS1* promoters in MV4-11 cells (Figure 2C and Figure S2B). Colocalization of AEP components with MLL oncoproteins was also observed on other MLL target genes, such as *CDKN1B* and *CDKN2C* (Milne et al., 2005), and the transcribed regions of *HOXA9* and *MEIS1* (Figures 2B and 2C), suggesting that MLL/AEP hybrid complexes may function in transcriptional elongation. Therefore, a subset of MLL oncoproteins results in consistent recruitment of AEP components at MLL target chromatin in leukemia cells.

Formation of a Higher Order MLL-AF5q31/AEP Hybrid Complex Is Required for Sustained Transcription of Target Genes and Transformation

AF4 and AF5q31 share extensive sequence similarity that resides in four subregions of the respective proteins (Figure 3A). A structure/function analysis (Figures 3B and 3C) revealed that: (1) P-TEFb interacts with AF4 and AF5q31 via subregion 1, which contains the N-terminal homology domain (NHD) (Nilson et al., 1997); (2) strong transactivation activity is conferred by subregion 2, consistent with previous observations (Prasad et al., 1995; Ma and Staudt, 1996; Morrissey et al., 1997); (3) ENL interacts with AF4 and AF5q31 through subregion 3 that encompasses the AF9 interaction domain (Srinivasan et al., 2004; Zeisig et al., 2005); and (4) the C-terminal homology domain (CHD) within subregion 4 mediates hetero-association of AF4 and AF5q31, which appears to be highly preferred over their respective homo-dimerization (Figure 3B). Preferential hetero-dimerization was also observed in co-IP experiments of endogenous or transfected MLL-AF5q31 (Figure 1E and

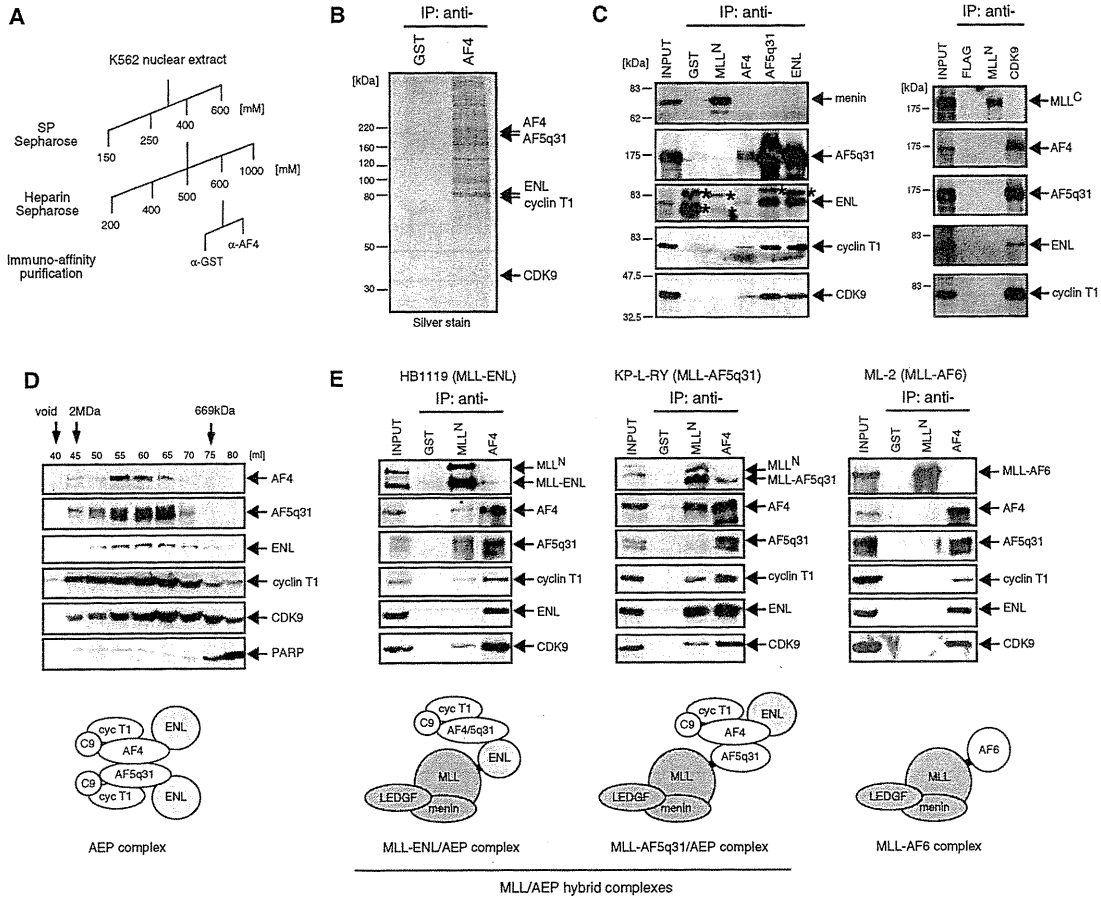

Figure 1. Heterologous Associations of Wild-Type and Oncogenic AF4 and ENL Family Proteins

(A) The scheme used for purification of the AF4 complex.

(B) A silver-stained image shows the proteins immuno-purified using anti-AF4 antibody and subsequently identified by mass spectrometry, as indicated by arrows on the right. Anti-GST antibody served as a negative control.

(C) K562 nuclear extracts were analyzed by IP western blotting. IP was performed with the antibodies indicated on the top, and the precipitates were immunoblotted with the antibodies indicated on the right. Anti-GST and anti-FLAG antibodies served as negative controls. Asterisks indicate signals from IgG used for IP.

(D) Selected fractions from gel filtration analysis of K562 nuclear extracts were analyzed by western blotting for AF4-associated factors (PARP served as a negative control). Molecular weight standards are shown on the top. A cartoon of a putative AEP complex is depicted. C9, CDK9; cyc T1, cyclin T1.

(E) IP western blot analysis was performed as in (C) on human leukemia cell lines that harbor MLL chromosomal translocations and express MLL chimeric oncoproteins (indicated at tops). Cartoons of putative MLL fusion complexes are depicted below. See also Figure S1.

Figure S3A), as well as an interaction assay based on GAL4-dependent transactivation (Figure S3B).

MLL fusion proteins containing the respective subregions of AF4 or AF5q31 were assessed for their oncogenic potentials in a myeloid progenitor transformation assay (Figure 3D) (Lavau et al., 1997). Only MLL-AF5q31 constructs containing subregion 4 (MLL-AF5-4 and MLL-AF5-34) induced serial replating activity and up-regulation of *Hoxa9* transcription (Figures 3E and 3F). This result indicates that none of the single functions (i.e., P-TEFb recruitment, transactivation, or association with ENL) is sufficient for transformation but rather CHD-mediated association with endogenous AEP is required. The corresponding MLL-AF4-4 and MLL-AF4-34 proteins were not stably expressed and thus unable to be evaluated (Figure 3F). Although recruitment of Enl was not sufficient for MLL-AF5q31-dependent transformation, Enl was required because its knockdown by sh-RNA substantially decreased the clonogenicity and *Hoxa9* expression of MLL-AF5q31-transformed cells (Figures 3G–3J). This phenotype was rescued by exogenous expression of human ENL, thus verifying the target specificity of the sh-RNA. Hence, formation of a higher order MLL/AEP hybrid complex on target genes is necessary for MLL-AF5q31-dependent transformation.

Transforming Properties of MLL-ENL and MLL-AF9 Correlate with Association with AF4 Family Proteins and DOT1L

A similar structure/function analysis of MLL-ENL demonstrated that C-terminal ENL residues (494–559) are required for the interaction with AF5q31 (Figures 4A and 4B). This region, which is evolutionally conserved with AF9 and *Saccharomyces cerevisiae*

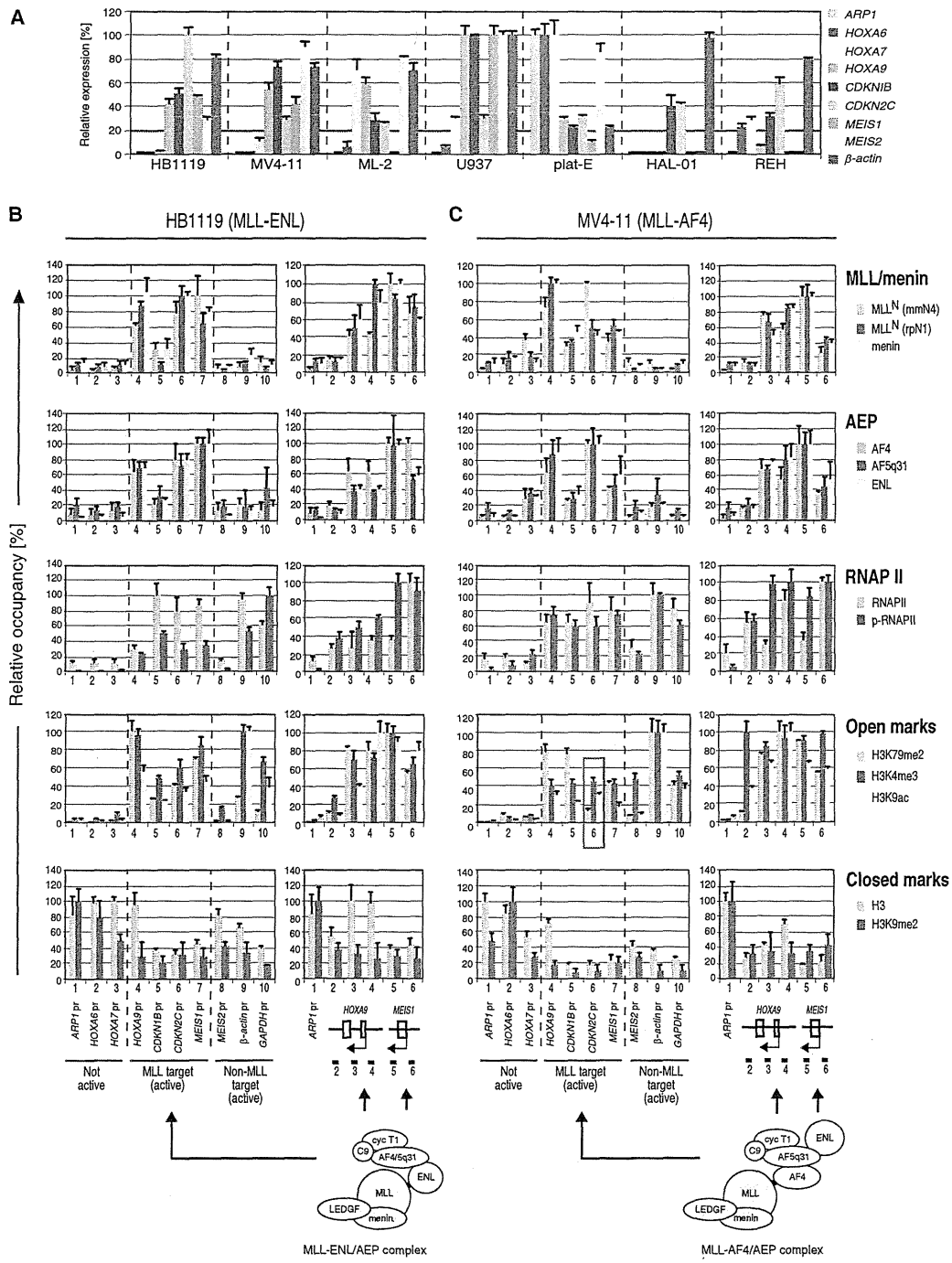

Figure 2. Colocalization of MLL Fusion Proteins and AEP Components on Chromatin

(A) Relative expression of various genes (indicated on the right) in seven human cell lines was analyzed by quantitative RT-PCR. Expression levels were normalized to *GAPDH* and are depicted relative to the highest value among the seven cell lines arbitrarily set as 100. Error bars represent standard deviations of triplicate PCRs.

(B) Genomic localizations of various proteins in HB1119 cells were determined by ChIP assay. Cross-linked chromatin was immunoprecipitated with antibodies specific for the indicated proteins and analyzed by quantitative PCR using primer/probe sets that target promoter-adjacent regions or other genomic regions indicated at the bottom. Occupancies are displayed relative to the highest value in the group arbitrarily set as 100. Error bars represent standard deviations of triplicate PCRs. Genes expressed more than 20% of the highest levels in (A) are defined as active genes.

(C) A comparable analysis as in (B) was performed for MV4-11 cells, which harbor a t(4;11) translocation and express MLL-AF4 proteins. The purple rectangle highlights a locus on which dimethyl H3K79 marks were absent, but the MLL-AF4/AEP complex was present. See also Figure S2.

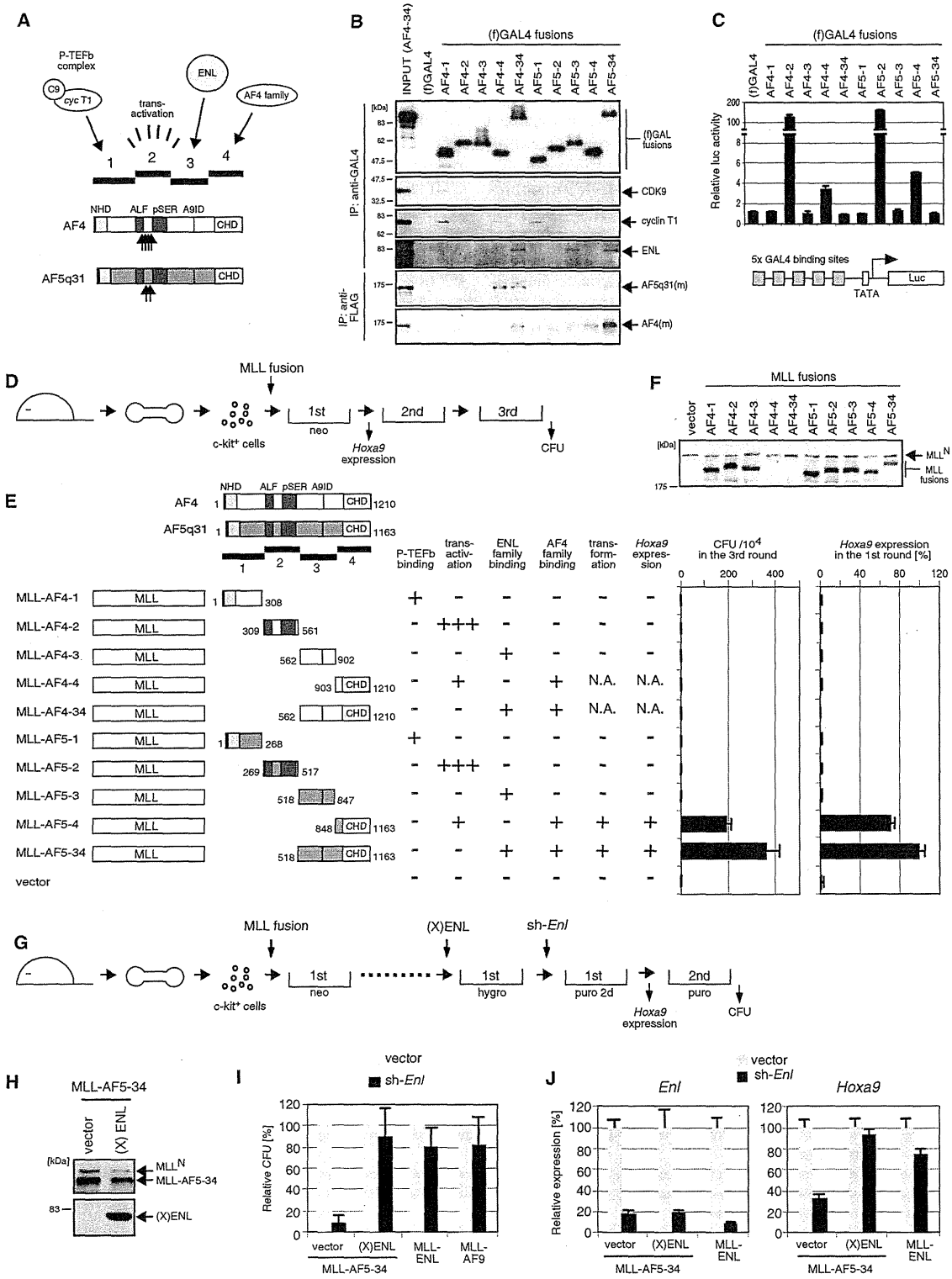
A
P-TEFb complex
C9
cyc T1
ENL
AF4 family
trans-activation
1
2
3
4
NHD
ALF
pSER
A9ID
AF4
CHD
AF5q31
B
INPUT (AF4-34)
(f)GAL4
(f)GAL4 fusions
AF4-1
AF4-2
AF4-3
AF4-4
AF4-34
AF5-1
AF5-2
AF5-3
AF5-4
AF5-34
[kDa]
IP: anti-GAL4
(f)GAL fusions
CDK9
cyclin T1
ENL
IP: anti-FLAG
AF5q31(m)
AF4(m)
C
Relative luc activity
5x GAL4 binding sites
Luc
TATA
D
MLL fusion
c-kit+ cells
1st
neo
2nd
3rd
Hoxa9 expression
CFU
E
P-TEFb binding
trans-activation
ENL family binding
AF4 family binding
trans-formation
Hoxa9 expression
CFU /10^4 in the 3rd round
Hoxa9 expression in the 1st round [%]
MLL-AF4-1
MLL-AF4-2
MLL-AF4-3
MLL-AF4-4
MLL-AF4-34
MLL-AF5-1
MLL-AF5-2
MLL-AF5-3
MLL-AF5-4
MLL-AF5-34
vector
MLL
N.A.
F
MLL fusions
vector
MLL^N
MLL fusions
G
MLL fusion
(X)ENL
sh-Enl
c-kit+ cells
1st
neo
1st
hygro
1st
puro 2d
2nd
puro
Hoxa9 expression
CFU
H
MLL-AF5-34
vector
(X) ENL
MLL^N
MLL-AF5-34
(X)ENL
I
vector
sh-Enl
Relative CFU [%]
vector
(X)ENL
MLL-ENL
MLL-AF9
MLL-AF5-34
J
vector
sh-Enl
Enl
Hoxa9
Relative expression [%]
vector
(X)ENL
MLL-ENL
MLL-AF5-34

Anc1 (designated AHD: Anc1 homology domain), displayed transactivation potential that correlated with association with AF4 family proteins (Figure 4C). The AHD of ENL also mediated association with DOT1L (Figure 4D), consistent with results of previous studies (Mueller et al., 2007). Mutations of MLL-ENL that abolished AF5q31 and DOT1L interaction (including a single L550E point mutation) resulted in failure to up-regulate *Hoxa9* transcription and transform myeloid progenitors (Figures 4E–4G). Similarly, the portion of AF9 retained in MLL-AF9 oncoproteins, which includes AHD (residues 502–568) (Figure 4A), mediated AF5q31 and DOT1L association and conferred GAL4-dependent transactivation, MLL-dependent *Hoxa9* expression, and myeloid transformation (Figures 4B–4G). Unlike MLL-AF5q31-transformed cells, MLL-ENL- and MLL-AF9-transformed cells did not require WT Enl because their clonogenicities were unaffected by its knockdown (Figures 3I and 3J), consistent with the observation that MLL-ENL did not form a complex with WT ENL in HB1119 cells (Figure 1E). These results suggest that association with AF4 family proteins and/or DOT1L is required for the oncogenic properties of MLL-ENL and MLL-AF9.

Interactions of ENL with DOT1L or AF4 Family Proteins Are Mutually Exclusive

To determine whether ENL can simultaneously coassociate with AF4 family proteins and DOT1L, IP analysis was performed on cells transiently expressing ENL, AF5q31, and DOT1L. Although ENL coprecipitated both AF5q31 and DOT1L, the latter two did not pull down each other (Figure 5A), indicating that the three proteins do not form a trimeric complex. Similarly, GAL4-AF5-3 effectively coprecipitated ENL but not DOT1L under conditions where GAL4-ENL successfully pulled down DOT1L (Figure S4). These data demonstrate that the associations of ENL family proteins with AF4 family proteins or DOT1L are mutually exclusive. Therefore, the ENL/DOT1L complex is a separate entity from AEP (Figure 5B).

Recruitment of AEP, versus DOT1L, Plays a Predominant Role in MLL-Dependent Leukemogenesis

The ability of MLL-ENL to associate with AF4 family proteins or DOT1L raised the issue of which interaction (MLL-ENL/AEP vs. MLL-ENL/DOT1L) is essential for leukemic transformation (Figure 5B). To address this issue, an artificial MLL fusion with DOT1L (MLL-DOT1L) that does not associate with AF4 (Figure 5C) but retains the HMT catalytic domain (thus mimics the MLL-ENL/DOT1L complex) was assessed for its transformation potential. MLL-DOT1L failed to sufficiently activate *Hoxa9* expression to immortalize myeloid progenitors (Figures 5D and 5E), despite the comparable levels of protein expression in packaging cells (Figure 5F) and mRNA expression in first-round colonies (Figure 5E). In the same experimental condition, MLL-AF5q31 successfully transformed myeloid progenitors (Figure 5E) without being able to directly associate with DOT1L (Figure 5C). These results, which contrast with those of previous studies (Okada et al., 2005), indicate that simple recruitment of DOT1L HMT activity alone to MLL target genes is not sufficient for transformation and support a more predominant role for AEP recruitment.

Nevertheless, DOT1L-dependent H3K79 methylation colocalized with the presence of MLL-ENL at all target loci tested in HB1119 cells (Figure 2B), indicating that not only AEP components but also DOT1L is consistently recruited by MLL-ENL. In MV4-11 cells, H3K79 methylation marks also colocalized at most of the MLL-AF4-occupied loci, consistent with previous observations (Krivtsov et al., 2008; Guenther et al., 2008), despite the apparent inability to directly recruit DOT1L (Figures 2C and 5C). However, the signal intensities of H3K79 dimethylation were relatively low at MLL-AF4-target loci, compared with those at MLL-ENL-target loci (compare relative intensities to those of *β-ACTIN* and *GAPDH*, which served as internal standards) (Figures 2B and 2C; Figure S2) and were minimal at the *CDKN2C* promoter in spite of the localization of abundant AEP components (Figure 2C, purple rectangle). Thus, DOT1L-dependent

Figure 3. Formation of an AEP-Like Complex Is Required for MLL-AF5q31-Dependent Myeloid Transformation

(A) The structures of AF4 and AF5q31 are schematically illustrated. Subregions (1–4) of AF4 and AF5q31 are indicated with associated functions. Upward arrows indicate the sites of fusion with MLL in human leukemia oncoproteins (Jansen et al., 2005) (A9ID, AF9 interaction domain; Srinivasan et al., 2004).

(B) The four subregions fused to GAL4 DNA binding domain were expressed in 293T cells (upper four panels) or coexpressed with myc-tagged AF4 or AF5q31 [AF4(m) or AF5q31(m)] (lower two panels) and analyzed by IP western blotting. IP antibodies are indicated on the left and proteins detected by western blotting are indicated on the right. (f)GAL4 fusions and myc-tagged AF4 family proteins were visualized with anti-FLAG and anti-myc antibodies, respectively.

(C) Transactivation activity of respective GAL4 fusions was analyzed using the reporter gene shown below. Error bars represent standard deviations from triplicate analyses.

(D) The experimental scheme of myeloid progenitor transformation assays to evaluate the oncogenic potentials of various MLL mutants shows the time points at which CFU (colony forming unit) activity or *Hoxa9* expression was examined.

(E) The structures of various MLL-AF4/AF5q31 mutants and their associated functions are summarized schematically. *Hoxa9* levels were normalized to *Gapdh* and displayed relative to *MLL-AF5-34*-transduced cells arbitrarily set at 100%. Error bars represent standard deviations of three independent analyses (left) or triplicate PCRs (right). N.A., not applicable because of unstable expression of MLL fusion proteins.

(F) Protein levels of respective MLL mutants in virus-packaging cells were examined by western blotting with anti-MLL^N antibody. MLL-AF4-4 and MLL-AF4-34 proteins were not stably expressed.

(G) The experimental scheme to evaluate the effect of *Enl* knockdown on MLL transformation is shown schematically. (X)ENL, Xpress-tagged human ENL.

(H) Transduced myeloid progenitors were analyzed by western blotting with anti-MLL^N (top) and anti-Xpress (bottom) antibodies to detect exogenous MLL-AF5q31 and human (X)ENL, respectively.

(I) The clonogenic potentials of MLL-AF5-34-transformed cells transduced with or without *(X)ENL* are shown at the second plating after sh-RNA transduction (vector or sh-*Enl*). MLL-ENL- or MLL-AF9-transformed cells were also subjected to sh-RNA transduction for comparison. CFUs are expressed relative to the vector control arbitrarily set as 100. Error bars represent standard deviations of three independent analyses.

(J) Cells from first-round colonies following sh-RNA transduction (vector or sh-*Enl*) were analyzed by RT-PCR for expression of endogenous *Enl* or *Hoxa9*. Expression levels were normalized to *Gapdh* and displayed relative to the vector/vector control cells arbitrarily set at 100. Error bars represent standard deviations of triplicate PCRs. See also Figure S3.

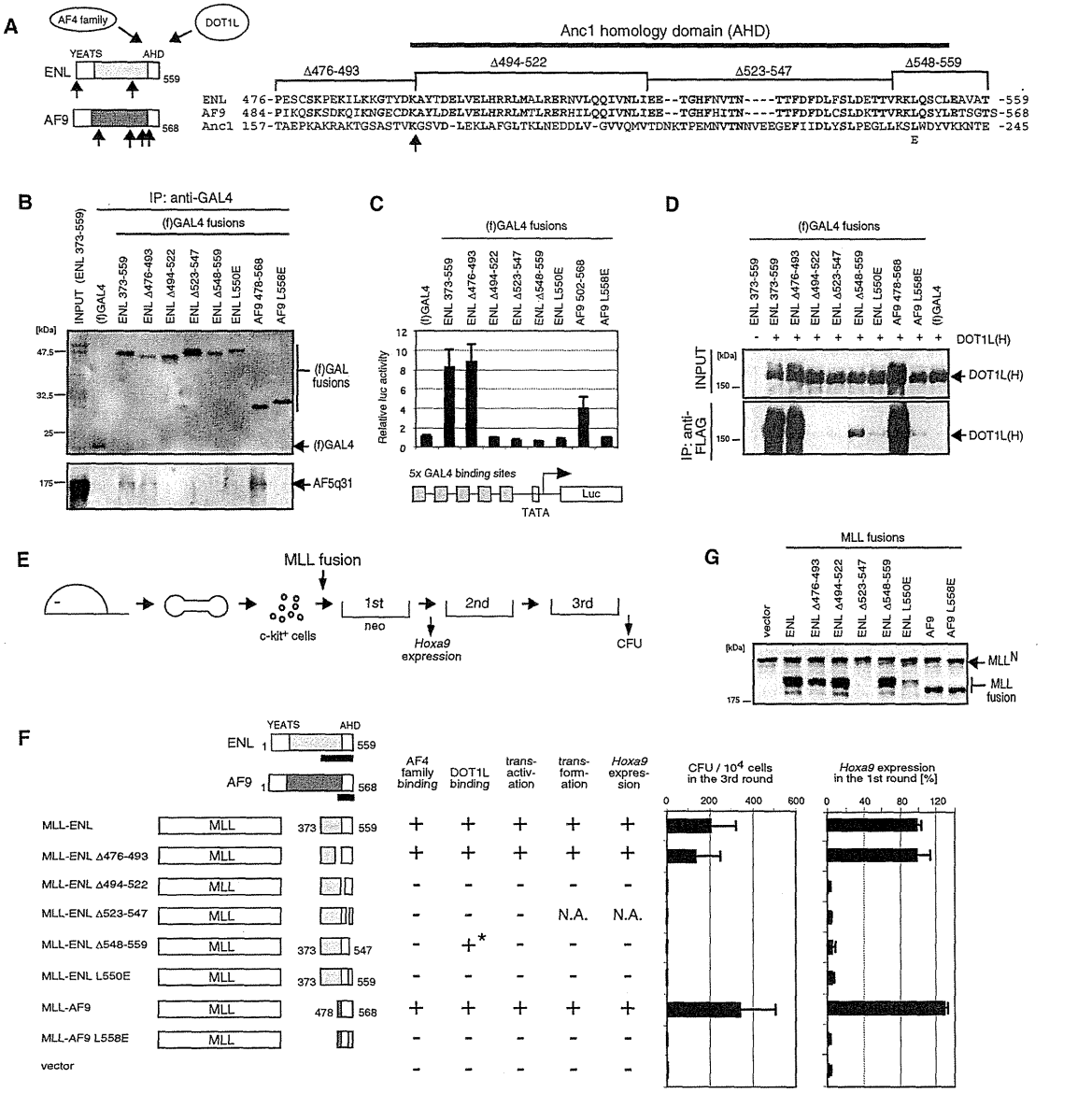

Figure 4. MLL-ENL and MLL-AF9 Transform Myeloid Progenitors via the AHD, which Is Responsible for Association with AF4 Family Proteins and DOT1L

(A) The structures of ENL and AF9 are schematically illustrated with associated functions (Zeisig et al., 2005). Aligned amino acid sequences for the minimum transformation domain are also shown with the positions of deletion or substitution mutations and AHD. Upward arrows indicate the sites of fusion with MLL in human leukemia oncoproteins (Jansen et al., 2005).

(B) Domain mapping of ENL family proteins for association with AF5q31 was performed with FLAG-tagged GAL4 fusion constructs of ENL (372–559 aa) and AF9 (478–568 aa). IP was performed with anti-GAL4 antibody, and the precipitates were immunoblotted with anti-FLAG antibody for (f)GAL4 fusions or anti-AF5q31 antibody for endogenous AF5q31.

(C) Transactivation activity of indicated GAL4 constructs was analyzed by luciferase assay as in Figure 3C.

(D) The same set of GAL4 fusion proteins used in (B) and HA-tagged DOT1L [DOT1L(H)] were coexpressed in 293T cells and analyzed by IP western blotting. IP was performed with anti-FLAG antibody and the precipitates were immunoblotted with anti-HA antibody.

(E) The experimental scheme is shown for myeloid progenitor transformation assays to evaluate the oncogenic potentials of MLL mutants.

(F) The structures of MLL-ENL and MLL-AF9 mutants and their associated functions are summarized with schematic representations. *Hoxa9* expression levels were normalized to *Gapdh* and displayed relative to the *MLL-ENL*-transduced cells arbitrarily set at 100%. Error bars represent standard deviations of three independent analyses (left) or triplicate PCRs (right). N.A., not applicable because of unstable expression of MLL fusion proteins. The asterisk indicates that association of ENL Δ548–559 mutant with DOT1L was detected but reduced substantially, compared with WT ENL.

(G) Protein levels of respective MLL mutants in virus packaging cells were examined by western blotting with anti-MLL^N antibody. MLL-ENL Δ523–547 was not stably expressed.

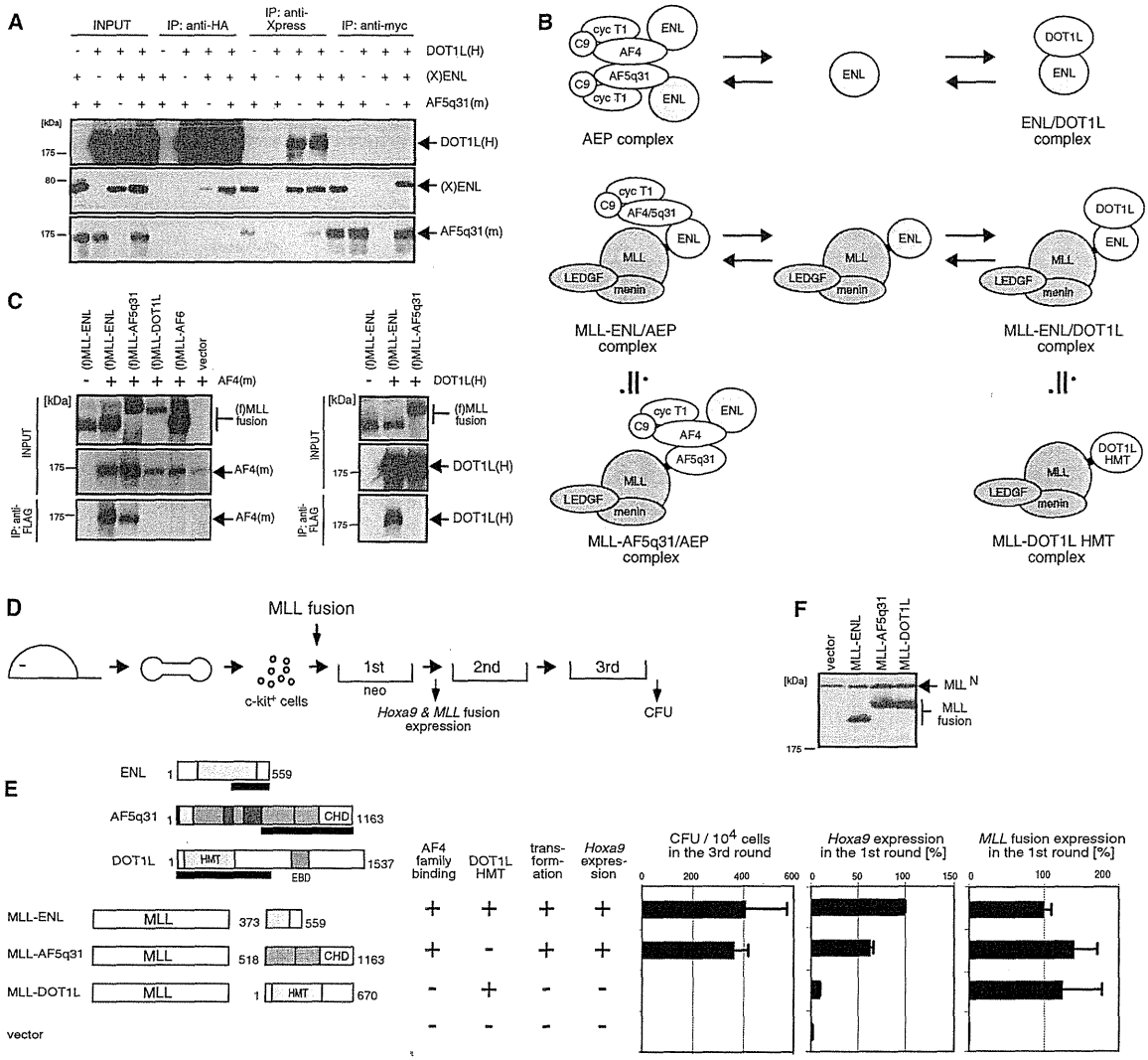

Figure 5. Associations of ENL Family Proteins with AF4 Family Proteins or DOT1L Are Mutually Exclusive

(A) AF5q31(m), (X)ENL, and DOT1L(H) were coexpressed in 293T cells and analyzed by IP western blotting. IP was performed with antibodies indicated on the top, and the precipitates were immunoblotted with anti-myc, anti-Xpress, or anti-HA antibody.

(B) Putative conformations of various ENL complexes are shown schematically. ENL forms two distinct complexes: AEP and ENL/DOT1L. Similarly, MLL-ENL participates in two mutually exclusive associations to form the MLL-ENL/AEP and MLL-ENL/DOT1L complexes that are approximate to the MLL-AF5q31/AEP and MLL-DOT1L complexes, respectively.

(C) FLAG-tagged MLL fusion proteins [(f) MLL fusions] were coexpressed with AF4(m) or DOT1L(H) in 293T cells and were analyzed by IP western blotting. IP was performed with anti-FLAG antibody, and the precipitates were immunoblotted with anti-MLL^N, anti-myc, or anti-HA antibody.

(D) The experimental scheme is shown for myeloid progenitor transformation assays to evaluate the oncogenic potentials of MLL mutants.

(E) The structures of MLL-fusion proteins and their associated functions are summarized. Expression of *MLL* fusion genes or *Hoxa9* was examined by RT-PCR in first-round colonies. Expression levels were normalized to *Gapdh* levels and are displayed relative to the transcript levels in *MLL-ENL*-transduced cells arbitrarily set at 100. Error bars represent standard deviations of three independent analyses (left) or triplicate PCRs (middle and right). HMT, histone methyltransferase catalytic domain; EBD, ENL binding domain (Okada et al., 2005; Mueller et al., 2007).

(F) Protein levels of MLL fusions in virus packaging cells were analyzed by western blotting with anti-MLL^N antibody. See also Figure S4.

H3K79 methylation is associated with the presence of the MLL-AF4/AEP-hybrid complex, but the two distinct biochemical entities are not constitutively coupled. These results suggest that DOT1L is functionally linked to MLL-AF4 but normally recruited to target loci subsequent to AEP components.

AEP Is Indirectly Recruited to MLL-AF6-Occupied Loci to Sustain Transcription and Transformation

To investigate whether AEP involvement is restricted to MLL fusions with AF4 and ENL family proteins, ChIP analyses were performed on ML-2 cells. Surprisingly, MLL-AF6 colocalized